Characterization of oligo(acrylic acid)s and their block co-oligomers

Adam T Sutton, R. Dario Arrua, Marianne Gaborieau, Patrice Castignolles, Emily F Hilder

Characterization of oligo(acrylic acid)s and their block co-oligomers

Adam T. Sutton[a,b], *R. Dario Arrua*[a,b], *Marianne Gaborieau*[c,d], *Patrice Castignolles*[c]*, *Emily F. Hilder*[a,b]*

[a] Future Industries Institute (FII), University of South Australia, Mawson Lakes, South Australia 5011, Australia

[b] Australian Centre for Research on Separation Science (ACROSS), School of Natural Sciences, University of Tasmania, Hobart, Tasmania 7005, Australia

[c] Western Sydney University, ACROSS, School of Science and Health, Locked Bag 1797, Penrith NSW 2751, Australia

[d] Western Sydney University, Medical Sciences Research Group, Locked Bag 1797, Penrith NSW 2751, Australia

AUTHOR INFORMATION

***Corresponding Author:**

Emily Hilder

E-mail: emily.hilder@unisa.edu.au

Tel/Fax: +61 8 8302 6292/+61 8 8302 0225

Patrice Castignolles

E-mail: p.castignolles@westernsydney.edu.au

Tel/Fax: +61 2 9685 9970/ +61 2 9685 9915

ABSTRACT

Oligo(acrylic acid), oligoAA are important species currently used industrially in the stabilization of paints and also for the production of self-assembled polymer structures which have been shown to have useful applications in analytical separation methods and potentially in drug delivery systems. To properly tailor the synthesis of oligoAA, and its block co-oligomers synthesized by Reversible-Addition Fragmentation chain Transfer (RAFT) polymerization to applications, detailed knowledge about the chemical structure is needed. Commonly used techniques such as Size Exclusion Chromatography (SEC) and Electrospray Ionization-Mass Spectrometry (ESI-MS) suffer from poor resolution and non-quantitative distributions respectively. In this work free solution Capillary Electrophoresis (CE) has been thoroughly investigated as an alternative, allowing for the separation of oligoAA by molar mass and the RAFT agent end group. The method was then extended to block co-oligomers of acrylic acid and styrene. Peak capacities up to 426 were observed for these 1D CE separations, 10 times greater than what has been achieved for Liquid Chromatography (LC) of oligostyrenes. To provide a comprehensive insight into the chemical structure of these materials ^{1}H and ^{13}C Nuclear Magnetic Resonance (NMR) spectroscopy was used to provide an accurate average chain and reveal the presence of branching. The chain length at which branching is detected was investigated with the results showing a degree of branching of 1 % of the monomer unit in oligoAA with an average chain length of 9 monomer units, which was the shortest chain length at which branching could be detected. This branching is suspected to be a result of both intermolecular and intramolecular transfer reactions. The combination of free solution CE and NMR spectroscopy is shown to provide a near complete elucidation of the chemical structure of oligoAA including the average chain length and branching as well

as the chain length and RAFT agent end group distribution. Furthermore, the purity in terms of the dead chains and unreacted RAFT agent was quantified. The use of free solution CE and ^{1}H NMR spectroscopy demonstrated in this work can be routinely applied to oligoelectrolytes and their block co-oligomers to provide an accurate characterization which allows for better design of the materials produced from these oligomers.

KEYWORDS. Oligomer, poly(acrylic acid), capillary electrophoresis, quantitative NMR spectroscopy, end group, degree of branching

Graphical Abstract

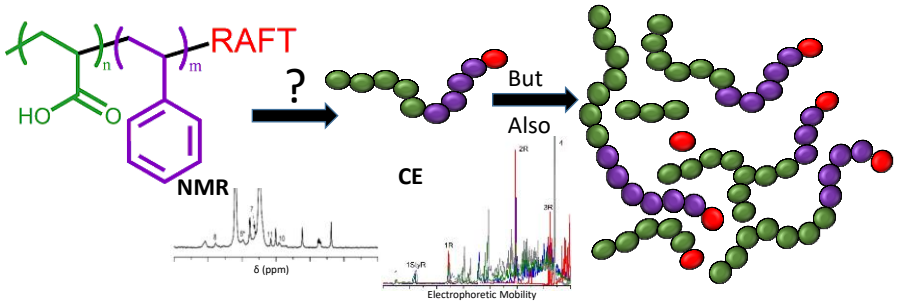

HIGHLIGHTS:

-Quantification of the degree of branching in oligomers

-9 monomer units is the shortest chain length where branching was detected

-Separation of oligo(acrylic acid) and its block co-oligomers according to chain length, end group and composition by free solution capillary electrophoresis

1. INTRODUCTION

Oligoelectrolytes have had growing interest in recent times with applications in controlled crystallization [1] and fuel cell membranes [2] amongst others. In particular oligomers of acrylic acid (oligoAA) are commonly used to synthesize amphiphilic block copolymers with a larger hydrophobic block. These block copolymers are currently used to produce latex

65 nanoparticles, [3, 4] anisotropic nanoparticles [5] and surfactants [6], e.g. to encapsulate
66 graphene oxide [7]. Block co-oligomers are block copolymers which contain short blocks,
67 typically with an average block length less than 10 monomer units long. Block co-oligomers
68 of oligoAA with styrene (Sty) or *n*-butyl acrylate synthesized by Reversible-Addition
69 Fragmentation chain Transfer (RAFT) polymerization [8] are currently used in industry as
70 pigment dispersants in paints [9, 10]. To properly design these block co-oligomers for these
71 applications careful attention to their chemical structure is required.
72
73 The chemical structure of oligoelectrolytes and their block co-oligomers vary in the
74 distribution of their block lengths, compositions and end groups. Size Exclusion
75 Chromatography (SEC) is commonly used to characterize oligomers although the separation
76 by hydrodynamic volume yields little to no information in terms of the composition and end
77 group distribution [11]. SEC of oligomers also suffers from poor resolution in terms of molar
78 mass due to the band broadening and the hydrodynamic volume being influenced by the end
79 group, composition and branching in addition to the molar mass [12]. Electrospray
80 Ionization-Mass Spectrometry (ESI-MS) can separate all chemical structures with different
81 molar masses, enabling the identification of most chemical structures present in an oligomer
82 sample [13, 14]. However, obtaining quantitative information from ESI-MS is difficult since
83 there is a bias in the ionization resulting in an underestimation of the average chain length
84 [15-17]. ESI-MS (direct infusion) was shown to underestimate the amount of control (RAFT)
85 agent by a factor of 25 [18]. ^{1}H Nuclear Magnetic Resonance (NMR) spectroscopy is
86 commonly used to determine the average chain length and composition, however, obtaining a
87 signal to accurately represent the end groups of the oligomer chains is difficult since there are
88 multiple end groups in the sample and their signals tend to overlap with other signals [11].
89 Liquid chromatography in the critical conditions, coupled with electrospray tandem mass

spectrometry (LCCC-MS/MS) has been used to assess the end groups of poly(ethylene oxide-*b*-Sty) block co-oligomers [19]. The critical conditions refer to separation independent from a polymeric sample's molar mass and have been sought without success for oligoAA based co-oligomers [20]. This is likely due to the difficulty in obtaining a purely size-exclusion separation mechanism and thus balancing the adsorption and exclusion of the oligomers is not possible. However, it is also important to note that these methods are unable to detect if there is any branching present in the oligomers. The potential for branching in oligomers is typically not acknowledged due to short chain length. Branching has been detected in poly(acrylic acid), PAA, obtained by radical polymerization using ^{13}C NMR spectroscopy as the quaternary carbon at the branching point has a distinct chemical shift at ~48 ppm [21-25]. Additionally, branching has been detected in polymers of hydrophobic acrylates synthesized using conventional or reversible-deactivation radical polymerization by ^{13}C NMR spectroscopy [26-29]. This contrasts with poly(methacrylic acid) which did not present any branching due to the absence of a hydrogen in the alpha position relative to the carbonyl group[30, 31]. The precision and accuracy of the quantification of the Degree of Branching (*DB*) in PAA has been recently assessed [32]. The presence of this branching is unintentional and due to transfer to polymer reactions. Branching is independent of a polymer sample's molar mass when the main source of branching is from intramolecular transfer to polymer (followed by propagation) [33-35]. Therefore, branching is potentially present in oligoAA which would influence the properties of their materials, such as the phase behavior, although branching is commonly assumed to be absent from oligoAA in the literature [36].

Free solution Capillary Electrophoresis (CE) is an alternative characterization technique for oligoelectrolytes since it separates molecules by their charge to friction ratio in an electrolyte solution. Free solution CE offers fast analysis of charged molecules with a low running cost,

typically less than chromatography methods used for the same analysis [37]. The use of free solution CE to characterize materials is increasing[38-40] with it being recently used to characterize biopolymers such as gellan gum[41] and chitosan[42, 43] as well as synthetic branched poly(acrylic acid)[21, 25], block copolymers,[44-46] nanoparticles[47] and nanodiamond[48]. It was previously demonstrated that free solution CE can separate oligoAA according to the chain length, end group and even tacticity [18, 49]. Although free solution CE has demonstrated superior resolution to SEC in terms of molar mass it is not commonly used to characterize oligoelectrolytes. Free solution CE has been shown to separate oligoelectrolytes, other than those of acrylic acid, such as oligo(sodium methacrylate)[18], oligonucleotides[50], oligo(styrene sulfonate)[51], gellan gum[41], oligo(acrylamido-*N*-propyltrimethylammonium chloride)[44], and aluminum chlorohydrateoligocations[52] according to their chain length. Thus there is great potential for free solution CE to become a common characterization method for oligoelectrolytes.

Herein we present a comprehensive characterization of oligoAA and their corresponding block co-oligomers, oligo(AA-*b*-Sty), using free solution CE and NMR spectroscopy. The separation conditions for oligoAA by SEC and free solution CE were examined to find the optimal method, with the free solution CE conditions also being assessed on the separation of oligo(AA-*b*-Sty). Furthermore the presence of branching in oligoAA was examined by ^{13}C NMR spectroscopy to estimate the shortest average chain length at which branching can be detected in poly(acrylic acid).

2. EXPERIMENTAL SECTION

2.1. MATERIALS

Milli-Q water was used in the synthesis and characterization. Acrylic acid (AA, Merck, ≥99 %) was purified by distillation under reduced pressure. Styrene (Sty, Sigma Aldrich, 99 %) was purified through an alumina column prior to use. The RAFT agent, 2-[[(butylsulfanyl)-carbonothioyl]sulfanyl] propanoic acid (PABTC), was synthesized as described previously.[36] HPLC grade acetone was obtained from Burdick & Jackson. 4,4-azobis(4-cyanopentanoic acid) (V-501, AR purity), 1,4-dioxane (ACS reagent, ≥99 %), tetramethylsilane (TMS, 99 %), sodium hydroxide (>98 %), lithium hydroxide monohydrate (AR purity), methanol (HPLC grade), ethanol (HPLC grade) and dimethyl sulfoxide (DMSO, >99 %) were purchased from Sigma Aldrich. Boric acid (≥98 %,) was obtained from BDH AnalaR, Merck Pty Ltd. Potassium hydroxide (85 %) was purchased from Chem-Supply. Sodium acetate (AR purity) and ammonium hydroxide (28-30 % aq.) were obtained from Ajax. Fused-silica capillaries (50 μm i.d., 360 μm o.d.) were obtained from Polymicro (Phoenix, AZ, USA). All deuterated solvents including 1,4-dioxane-d_8 (99 % D), deuterium oxide, (D_2O, 99.9 % D), 40 % sodium deuteroxide in D_2O (99.5 % D), tetrahydrofuran-d_8 (THF-d_8, 99.5 % D) and DMSO-d_6 (99.9 % D) were sourced from Cambridge Isotope Laboratories, Inc.

2.2. SYNTHESIS

OligoAA samples were synthesized as described previously.[18] The first block of oligoAA (targeting 5 units of AA) was synthesized by adding 0.33 g (1.39×10^{-3} mol) of PABTC RAFT agent, 0.50 g (6.96×10^{-3} mol) of acrylic acid, 0.04 g (1.39×10^{-4} mol) of V-501 and 5 mL of dioxane to a round bottom flask. After purging the mixture with argon for 10 min, the mixture was left for 2 h at 60 °C under an argon atmosphere while stirring. After this time the reaction was stopped and the flask removed from the oil bath. Styrene was then added to create the second block, when 1 styrene unit was targeted 0.14 g (1.39×10^{-3} mol) was used.

The mixture was again purged with argon for 10 min and the second polymerization step was performed at 60 °C overnight under an argon atmosphere while stirring. Dioxane was partially removed under reduced pressure, the yellow viscous oil was then dissolved in 5 mL of acetone and then dried under vacuum to yield a yellow solid. Samples are listed in Tables 1 and S-1, with the sample codes AAy and AAyStyz where average chain length is y AA monomer units and z Sty monomer units.

2.3. SIZE EXCLUSION CHROMATOGRAPHY

The experimental set up was the same as previously described[11] except in some cases where 0.1 % (w/w) trifluoroacetic acid (TFA) was used instead of 5.0 % (w/w) acetic acid as described in the text.

2.4. CAPILLARY ELECTROPHORESIS

Typically experiments involving oligoAA were conducted using an Agilent ^{3D}CE instrument with the experimental parameters previously described for alkali borate[49] and for ammonium acetate[18] background electrolytes (BGE), which were prepared to pH 9.2 with varying concentrations. Other specific information details are provided in figure captions. When an organic solvent was added to the BGE, it was added such that the concentration was 10 % (v/v).

Block co-oligomers and their precursor, AA4, were analyzed as follows. Experiments were conducted using an Agilent 7100 CE instrument (Agilent Technologies, Waldbronn, Germany) with a Diode Array Detector (DAD) monitoring at 200 and 290 nm with 10 and 20 nm bandwidths, respectively. The samples were dissolved at 5 g L^{-1} in water containing 1 mol equivalent of 1 M NaOH with respect to the acrylic acid monomer units. 10 µL of 10 %

189 (v/v) DMSO was added to each 400 µL sample to mark the electroosmotic flow (EOF). A
190 400 mM sodium borate buffer at pH 9.2 was used as the background electrolytes (BGE).
191 Buffers were sonicated for 5 min and filtered before use with a 0.2 µm, poly(vinylidene
192 fluoride) filter. Samples were injected hydrodynamically by applying 30 mbar of pressure for
193 10 s. Separations were performed at 30 kV and 25 ºC in a fused-silica capillary with a total
194 length of 59.2 cm (effective length 50.7 cm). The capillary was pre-treated prior to use by
195 flushing for 10 min with 1 M NaOH, for 5 min with 0.1 M NaOH, for 5 min with water and
196 for 5 min with the BGE. Preconditioning between injections involved a 2 min flush with 1 M
197 NaOH followed by a 5 min flush with the BGE. After the last electrophoresis experiment, the
198 capillary was flushed for 1 min with 1 M NaOH, for 4 min with 0.1 M NaOH, for 10 min
199 with water and for 10 min with air. Data was acquired using Chemstation A.10.01. The
200 migration time was converted to electrophoretic mobility for universal comparison of the
201 separations (Equation S-1 in supporting information), the absorbance was converted into the
202 weight-distribution of electrophoretic mobilities, $W(\mu)$, according to reference[53] (Equation
203 S-2), the data was then plotted and integrated using OriginPro 8.5. To improve the precision
204 of the electrophoretic mobility the distributions for the block co-oligomers and their
205 precursors were corrected, using Equation S-3, to the electrophoretic mobility of the peak
206 AA4 without the RAFT agent end group, which was 4.70×10^{-8} $m^2V^{-1}s^{-1}$ (1.67 % *RSD*,
207 n=16).
208
209 2.5. NMR SPECTROSCOPY
210 One-dimensional (1D) experiments for signal identification of AA3, AA5, AA6, AA9, AA10
211 and AA21 were conducted at 25 °C on a Bruker DRX500 spectrometer (Bruker Biospin Ltd,
212 Sydney) equipped with a TIXS probe and operating at Larmor frequencies of 500 MHz and
213 125 MHz for ^1H and ^{13}C, respectively. Samples were dissolved in D_2O at 100-170 g L^{-1}. ^1H

214 NMR spectra were recorded with a 45° flip angle, 32 scans and a 4 s repetition delay. ^{13}C
215 NMR spectra were obtained with a power-gated decoupling pulse sequence with a 45° flip
216 angle, 18,000 scans and a 2 s repetition delay. DEPT-135 ^{13}C NMR spectra were recorded
217 with 12,000 scans and a 3 s repetition delay.
218
219 Quantitative ^{13}C NMR spectra for samples AA9, AA10 and AA21 were obtained at room
220 temperature with a Bruker Avance 400 spectrometer (Bruker Biospin Ltd, Sydney) equipped
221 with a 5 mm BBO probe and operating at Larmor frequencies of 400 MHz and 100 MHz for
222 ^{1}H and ^{13}C, respectively. Samples were dissolved in D_2O at 143 to 155 g L^{-1}. An inverse
223 gated decoupling pulse sequence was used. The repetition delays were set at least five times
224 longer than the longitudinal relaxation times (T_1) of the signals of interest in order to ensure
225 that the spectra obtained in this study were quantitative. T_1 values were overestimated for
226 each sample using the one-dimensional inversion recovery pulse sequence (see supporting
227 information sections 5.2 and 6.1 containing Figure S-15 to S-21). A repetition delay of 15 s
228 was found to be longer than $5T_1$ thus sufficient to make all signals from the sample
229 quantitative except those corresponding to the carbonyl region. For samples AA9, AA10 and
230 AA21 spectra were obtained with 15,008, 3,360 and 15,360 scans, respectively.
231
232 1D NMR spectra for block co-oligomers, AA4Sty1, AA4Sty2 and AA4Sty3, and their
233 precursor, AA4, along with 2D NMR spectra were recorded using a Bruker DRX300
234 spectrometer (Bruker Biospin Ltd, Sydney) equipped with a 5-mm dual 1H/13C probe, at
235 Larmor frequencies of 300.13 MHz for ^{1}H and 75 MHz for ^{13}C. Samples were dissolved in a
236 deuterated solvent (four different solvents were used, see captions of the relevant figures) at
237 10 g L^{-1} for ^{1}H NMR spectra, at 200 g L^{-1} for ^{13}C NMR and 2D spectra of oligoAAs, and at
238 100 g L^{-1} for ^{13}C NMR and 2D spectra of block co-oligomers . Spectra were recorded at 20

°C except when D_2O and NaOD were used as the solvent in which they were recorded at 60 °C. ^{1}H NMR spectra were recorded with a 45° flip angle, 128 scans and a spectral width of 10,000 Hz. ^{13}C NMR spectra were acquired using an inverse-gated decoupling pulse sequence with a 90° flip angle, 6,000 scans and a spectral width of 20,000 Hz. ^{13}C DEPT-135 spectra were recorded using the same conditions except for 90° and 180° ^{13}C flip angles, as well as a 135° ^{1}H flip angle. The repetition delay of 25 s was found to be greater than $5T_1$ for all signals in both ^{1}H and ^{13}C experiments for samples dissolved in dioxane-d_8, THF-d_8 and D_2O with 1 mol equivalent of NaOD, except the signals corresponding to the solvent and the carbonyl of the residual acrylic acid monomer (see section 6.1 in supporting information).

^{1}H-^{1}H COrrelation SpectroscopY (COSY) spectra were acquired using the Bruker 'cosyqf' pulse sequence. The spectral width was 3,000 Hz in both dimensions. 2,048 increments were recorded in the direct dimension and 256 increments in the indirect dimension. The repetition delay between scans was 1 s. The ^{1}H-^{1}H COSY spectra were plotted with a 4,096 × 512 increment matrix. ^{1}H-^{13}C Heteronuclear Multiple-Quantum Correlation (HMQC) spectra were acquired using the Bruker 'hmqcgpqf' pulse sequence. The indirect dimension (^{1}H) had a spectral width of 3,000 Hz with 2,048 increments, while the direct dimension (^{13}C) had a spectral width of 15,100 Hz with 128 increments. The repetition delay between scans was 1 s. ^{1}H-^{13}C HMQC spectra were plotted with a 1,024 × 1,024 increment matrix.

For spectra recorded in dioxane-d_8 the ^{1}H and ^{13}C chemical shift scales were referenced to solvent signals at 3.53 and 66.48 ppm, respectively (these values were determined from measurements of dilute TMS in dioxane-d_8, in which the TMS signals were set to 0 ppm). For spectra recorded in DMSO-d_6 and THF-d_8 the chemical shift scales were referenced to the solvent signals at 2.50 ppm and 3.58 ppm, respectively, for ^{1}H and at 39.52 ppm and 67.21

ppm, respectively, for ^{13}C NMR spectra [54]. For spectra recorded in D_2O with or without NaOD, ^{1}H and ^{13}C chemical shift scales were externally calibrated with the resonance of the methyl signal of ethanol in D_2O at 1.17 and 17.47 ppm, respectively [54].

3. RESULTS AND DISCUSSION

3.1. OPTIMIZING SIZE EXCLUSION CHROMATOGRAPHY (SEC) SEPARATIONS

Free solution CE was previously shown to have a far higher resolution than aqueous or organic SEC routinely used for oligo or poly(acrylic acid) [49]. Aqueous SEC[31] exhibited a poorer resolution than tetrahydrofuran SEC with 5 (w/w)% acetic acid as additive[36, 49] in the case of oligoacrylates. However, SEC is still normally the first technique used to characterize oligomers, hence, we attempted to improve the resolution further. The SEC resolution was improved by using 0.1 (w/w)% TFA (instead of 5 (w/w)% acetic acid)[55] enabling the quantification of the unreacted RAFT agent between 28 and 30 min (Figure 1), the details are more heavily discussed in the supporting information section 1. However, the improved SEC resolution is still far lower than the resolution obtained by free solution CE.

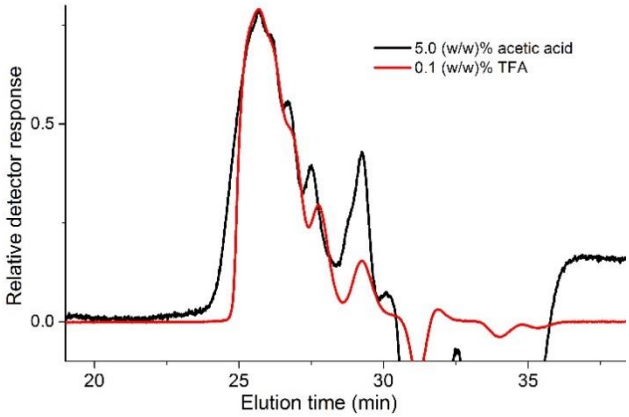

Figure 1. Comparison of SEC separations of AA5 using a THF mobile phase containing 5 (w/w)% acetic acid (black), or 0.1 (w/w)% TFA (red). Injection concentrations were 1.1 g L^{-1} and 0.2 g L^{-1}, respectively.

3.2. DISSOLUTION

The first step in any liquid-state analysis is usually the dissolution of the sample. OligoAA and their block co-oligomers are challenging to fully dissolve since the sample contains molecules with a range of hydrophobicities, in particular when the PABTC RAFT agent in used. In the case of branched PAAs[32] and starch[56], solution-state ^{1}H NMR showed that complete dissolution cannot always be determined by visual inspection and this can be expected also for other oligomers and polymers [56]. CE has been shown to be able to monitor dissolution and compared to solution-state ^{1}H NMR spectroscopy in the case of chitosan.[57] In addition, (some) aggregates can be detected by CE as sharp peaks.[41, 57] Therefore the dissolution of oligoAA was monitored by free solution CE using DMSO as an internal standard, as only the soluble fraction is detected (Figures S-1 and S-2). In particular the RAFT agent peak area was monitored as it is the most hydrophobic component of an oligoAA sample and thus the most challenging to dissolve in aqueous solvents. It was found to take approximately 10 h for all the unreacted RAFT agent to dissolve (Figure S-1) and that this dissolution does not follow a first-order kinetics (Figure S-3). No degradation was detected after 9 days in solution.

In the case of a free solution CE analysis it is possible to have the sample in solvent completely different to the BGE. Dissolving the samples in the BGE (Figure S-7a) or dilute NaOH (Figure 2b) both provided effective separations, while when dissolved in dioxane, the dioxane was adsorbing on the capillary wall and reducing the peak efficiency as many peaks presented shoulders (Figure S-4) when compared to the separation when dissolved in an aqueous solvent. The effect of the solvent used for the dissolution of oligoAA for ^{1}H NMR analysis is shown in Figure S-5 and discussed in section 2.2 of the supporting information.

3.3. OPTIMIZING FREE SOLUTION CAPILLARY ELECTROPHORESIS (CE) SEPARATIONS

The previous free solution CE separations of oligoAA showed that it is possible to have baseline resolution of chains up to three units long [18]. The longer chain lengths have a similar electrophoretic mobility preventing their separation, thus making the determination of the complete molar mass distribution difficult. However, it is possible to obtain the molar mass distribution of oligomers using CE with MS and UV detection (CE-MS), since the MS can identify the molar mass at each point. To achieve the previous selectivity the separation took place in approximately 30 min. Therefore additional experimentation was conducted to further improve the resolution while achieving a higher throughput.

Performing a free solution CE experiment is fairly simple but finding optimal conditions can be tedious since a number of variables can be changed such as the type of BGE, concentration of BGE, length of capillary, capillary surface, etc. Here we have examined a number of experimental conditions to determine the optimal conditions for a required separation.

Borate buffers are commonly used as a BGE in free solution CE due to the robustness, low cost and longevity. Furthermore the pH range of borate buffers (pH 8.2-10.2) ensures that oligoelectrolytes with a pK_a lower than this pH are predominately in the charged state.

Previous attempts to separate PAA with free solution CE at physiological pH led to irreproducible separations, thus lower pHs were not assessed for the separation of oligoAA [58]. Different counter ions can be used to alter the separation performance. Potassium and sodium counter ions gave similar selectivity, while a lithium counter ion led to a similar selectivity for chains with less than 3 monomer units but a reduced selectivity for the larger molar mass chains (Figure S-6). The electrophoretic mobility decreases with the size of the counter ion, consistent with the dependence of the protonation constants of polyacrylates with these counter-ions: $Li^+ > Na^+ \geq K^+$[59]. The lower electrophoretic mobility resulted in a faster separation. Free solution CE of polyelectrolytes follows the same trend that once they reach a certain chain length their electrophoretic mobility and thus separation becomes independent of chain length, therefore we refer to this mode of free solution CE as Capillary Electrophoresis in the Critical Conditions (CE-CC) in analogy to its namesake in liquid chromatography[60]; details can be found in a review [38]. The loss of resolution for the higher molar masses when using lithium in the BGE suggests that the critical conditions are reached earlier than when using other counter ions. This is beneficial for analyzing polyelectrolytes but in the case of oligoelectrolytes it provides less resolution. The overall separation time is faster with a lithium borate buffer so when only quantifying the low molar mass substances such as the unreacted RAFT agent using lithium is useful. A disadvantage of borate buffers is that they are not MS compatible, therefore to ensure the same separation is possible in an MS compatible BGE ammonium acetate was also examined. Ammonium acetate provided a resolution slightly higher than the borate buffers (Figure S-6). Therefore, high resolution separation of oligoelectrolytes with MS identification is possible. The disadvantage of using ammonium acetate is that its volatile nature prevents its storage and limits its longevity.

Increasing the BGE concentration improves the resolution at the cost of separation time (Figure S-7). The electrophoretic mobility of the oligoAA decreased with increasing BGE concentration as expected [61]. A 400 mM sodium buffer was typically the maximum concentration that could be used to create high and stable electric fields of 500 V cm^{-1}. This BGE and electric field provided very high resolution as separation by the tacticity of chains with 3 AA units could be achieved, as discussed previously[18], with a total separation time of 30 min in a 40 cm capillary. At half the BGE concentration the separation took place in 10 min.

Two different capillary lengths were examined, 40 cm and 100 cm, using 200 mM lithium borate and 100 mM ammonium acetate as BGEs. The longer capillary shows a strong improvement in the resolution with a greater number of peaks visible and narrower peaks (Figure S-8). The separation by tacticity of the oligomer chain with 3 monomer units is visible with both BGEs further showing the improvement in resolution, but the improved resolution comes at the cost of separation time. The longer capillary led to a 6 to 10 times longer separation as shown with two BGEs (Figures S-6d and 8).

375 Table 1. Average chain length and composition, RAFT agent conversion and average degree of branching of oligoAA and oligo(AA-

376 *b*-Sty) samples.

Sample code	Theoretical chain length[a]	Chain length at maximum of ESI-MS distribution[b]	Number-average chain length by NMR[c]		Number-average chain length of living chains[e]		Sty fraction[f]		Degree of Branching (%)[h]	Weight of RAFT agent remaining (% w/w)[i, j]	Conversion of RAFT agent (% mol/mol)[k]		Blocking efficiency (%)[m]
			^{1}H[d]	^{13}C[d]	^{1}H[d]	^{13}C[d]	theoretical	^{1}H NMR[g]	^{13}C NMR[d]		Free solution CE[i, l]	^{1}H NMR[d]	^{1}H NMR[d]
AA21	15.00	16	ND[n]	20.65 ± 0.38	ND	17.44 ± 0.32	-	-	2.8 ± 0.5	<LOD[o]	100	ND	-
AA9	7.52	8	ND	9.30 ± 0.73 [9.61 ± 0.10[p]]	ND	8.30 ± 0.08	-	-	1.0 ± 0.4	0.28 ± 0.01	99.5± 0.1	ND	-
AA4	5.62	ND	4.62 ± 0.03	3.70 ± 0.40 [4.64 ± 0.04[p]]	3.36 ± 0.03	3.36 ± 0.04	-	-	<LOD	7.47 ± 0.68	86.0 ± 0.9	90.6 ± 0.1 (88.9 ± 16.0[q])	-
AA4Sty1	6.62	ND	5.45 ± 0.08	ND	4.29 ± 0.06	ND	0.15	0.15	<LOD	2.09 ± 0.03	NP[r]	95.7 ± 1.3	51.6 ± 0.6
AA4Sty2	7.62	ND	5.74 ± 0.10	ND	5.37 ± 0.09	ND	0.26	0.27	<LOD	2.45 ± 0.01	NP	NP	62.6 ± 9.0
AA4Sty3	8.62	ND	6.26 ± 0.02	6.34 ± 0.58	5.67 ± 0.02	5.75 ± 0.53	0.35	0.35(0.37 ± 0.02[d,q])	<LOD	1.43 ± 0.26	NP	NP	73.3 ± 1.3

[a]Calculated using Equation S-8[62] [b]values published previously[18] [c]calculated using Equations S-10 to S-17 [d]error calculated from the *SNR* using Equation S-9 [e]calculated using Equations S-10 to S-13 with the numerator multiplied by the weight fraction of monomer units in living chains shown in Table 3 [f]total Sty content of sample not ratio in block co-oligomer, calculated using Equations S-19 to S-21 [g]error from *SNR* was <1.5 % [h]calculated using Equation 2 [i]determined by free solution CE with n=3 for oligoAA and n=2 for oligo(AA-*b*-Sty) [j]absorbance at 200 nm to measure the weight fraction calculated using Equation S-5 [k]calculated by the unreacted RAFT/total RAFT ×100 [l]absorbance at 290 nm to measure the RAFT agent, value calculated using Equation S-5 [m]calculated by Sty units adjacent RAFT/all monomer units adjacent RAFT ×100 [n]ND stands for not determined [o]LOD stands for limit of detection [p]calculated using Equations S-16 and S-17 which also uses H terminated end group, the error was calculated using Equation S-18 [q]determined from ^{13}C NMR spectroscopy [r]NP stands for not possible due to signals not being resolved from other units and Sty units also absorbing at 290 nm.

In free solution CE the migration of the ions is due to the attraction to the electrodes and the Electro-Osmotic Flow (EOF). Reducing the EOF has been shown to improve the resolution of CE previously [63, 64]. The strength of the EOF is proportional to the surface charge of the capillary, thus the migration speed can be controlled by altering the surface charge of the capillary. Different coatings were trialed with the details of these separations discussed more heavily in the supporting information section 4.3 and shown in Figures S-9 to S-13. In summary, a C18 coating was the best of the coatings trialed to reduce the EOF which resulted in longer separation times with minimal improvement in the resolution.

An alternative means of reducing the EOF is to add an organic modifier to the BGE, although this also changes the solvation of the analytes and so could change their selectivity. Acetone or methanol are miscible with the BGEs used and can dissolve oligoAA and its more hydrophobic block co-oligomers. 10 % (v/v) of acetone in the BGE prevented a stable electric field while methanol had the desired effect of reducing the EOF. The use of 10 % (v/v) of methanol in the ammonium acetate buffers did not show any significant change in the resolution. However, using the same concentration in a lithium borate buffer yielded an improvement in the resolution of the higher molar masses (Figure S-14). The methanol caused the EOF marker to migrate 0.5 min slower than without methanol which resulted in the separation taking 25 min instead of 13 min. However, the methanol did not provide baseline separation of the oligomer chains greater than 3 monomer units long, which was achieved with a lithium borate buffer with a longer capillary.

Depending on the desired characterization the different free solution CE conditions can be used. In some cases the optimal resolution is desired but in some circumstances such as monitoring the

conversion of the RAFT agent (or monomer conversion measurement) minimal resolution and fast separation time is preferred, which was possible with free solution CE with separations taking place in less than 5 min (Figure 2a). Currently no chromatography method is available to separate RAFT agents or other chain transfer agents from other components of a polymer sample. Therefore the efficiency and robustness of free solution CE enables the monitoring of chain transfer agents. The recommended free solution CE BGE and capillary length to obtain the required information is summarized in Table 2. To obtain the optimal resolution it requires a balance of different conditions. The separation of oligomer chains that were 4 units long was only possible with long capillaries or with a BGE not containing lithium with concentrations at least 400 mM, thus the recommended conditions for optimal resolution are using a 400 mM sodium borate buffer as the BGE in a 60 cm total length capillary (Figure 2b). It may be possible to further improve the resolution with longer capillaries and more concentrated BGEs but this would require exorbitantly long separation times greater than 60 min. For oligoelectrolytes other than oligoAA it may be necessary to use MS detection for peak identification. Similar resolution is obtained using 150 mM ammonium acetate which can be used in conjunction with MS detection for peak identification. The variety of free solution CE conditions allows for a range of oligoelectrolytes to be analyzed.

433 Table 2. Recommended conditions for different goals: BGE and capillary length (total length l_t,
434 effective lenght l_d) for the analysis of oligoAA by free solution CE, with approximate separation
435 time.

Goal	BGE	l_t [l_d] (cm)	Approx. time (min)†
Optimal resolution	400 mM sodium borate	60[51.5]	60
Unreacted RAFT agent	100 mM lithium borate	35[26.5]	3
Couple to MS	150 mM ammonium acetate	100[91.5]	40
Hydrophobic samples	100 mM sodium borate with 10 %(v/v) methanol	40[31.5]	25

436 † time for last peak to be detected

437

438

439

440

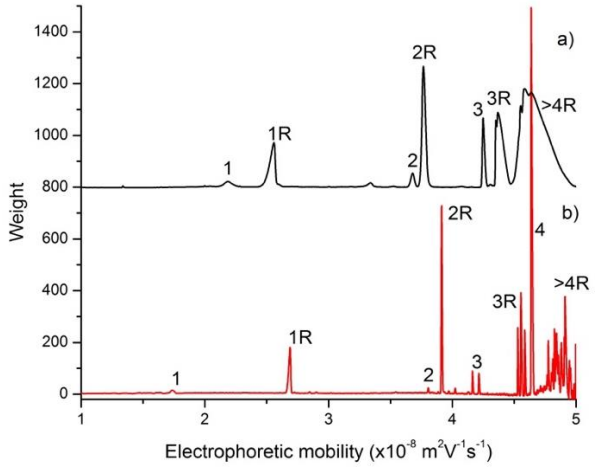

441

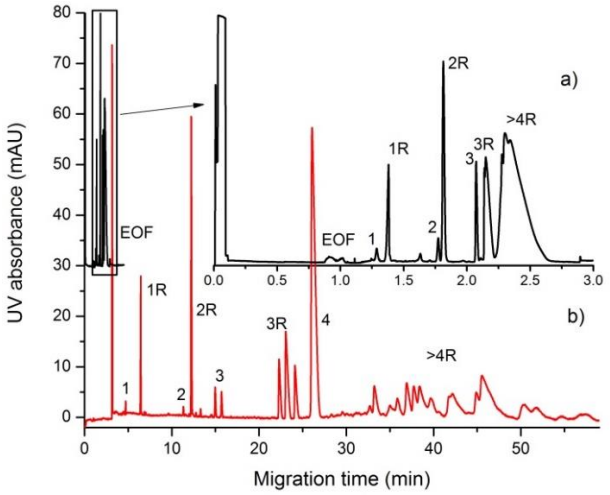

442

443 Figure 2. Separations of oligoAA to provide the fastest separation (black, 100 mM lithium borate
444 buffer, 40 cm total length capillary, 31.5 cm effective length, injection concentration 1 g L^{-1}) and
445 optimal resolution (red, 400 mM sodium borate buffer, 59.2 cm total length capillary, 50.7 cm
446 effective length, injection concentration 5 g L^{-1}). Electropherograms are shown as a function of
447 electrophoretic mobility (top) and migration time (bottom). Separations took place at 25 °C and
448 30 kV, detection at 200 nm. Numbers indicate the number of monomer units while R indicates
449 the presence of a RAFT agent end group.

450

The performance of a separation can be measured in terms of its peak capacity (N_c), which indicates the number of peaks that can be baseline separated over the time of the separation. Using the RAFT agent peak as a reference, since it is baseline separated in all free solution CE conditions, the N_c of the free solution CE measurement was estimated using Equation S-4. For the fastest separation conditions (Figure 2a) a N_c of 47 was estimated while for the most resolved conditions (Figure 2b) the N_c was 426. The N_c of one-dimensional reversed phase liquid chromatography to separate oligoSty was found to be 38 and 45 for different separation conditions.[65] Therefore the efficiency achieved by free solution CE for oligomers is far higher than that of other separation methods. Due to the high N_c of free solution CE more information regarding the purity and livingness of oligoAA can be determined than with any other separation method. Furthermore in a block co-oligomer sample there are hundreds of different molecules, thus higher resolution and peak capacity separations are needed to obtain a clearer understanding of the heterogeneity of a sample's chemical structures.

3.4. NUCLEAR MAGNETIC RESONANCE (NMR) SPECTROSCOPY SIGNAL ASSIGNMENT

Oligomer samples may possess a number of different chemical structures as shown in Figure 3. With a thorough NMR signal assignment accurate chemical structures can be obtained. The signal assignment of ^{1}H and ^{13}C NMR spectra of oligoAA and oligo(AA-*b*-Sty) is shown in Figures 4 to 6. A detailed description of how the signals were assigned is provided in the supporting information section 5.1. In addition 1D and 2D NMR spectra used for the signal assignment are shown in Figures S-22 to S-31.

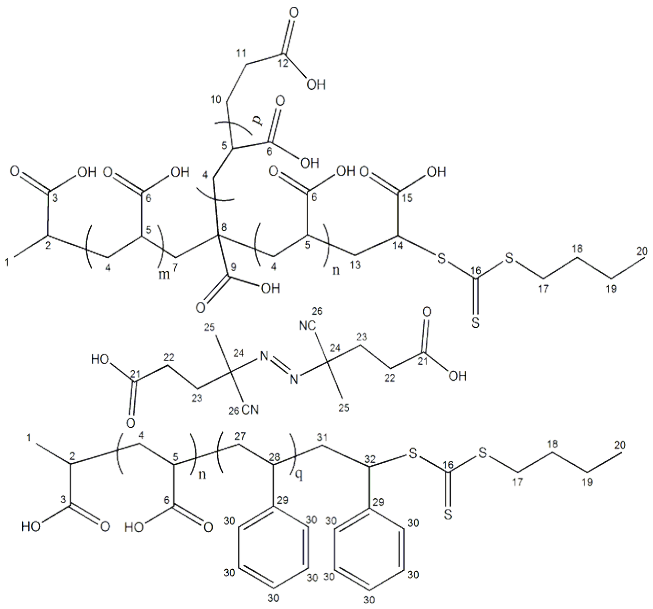

Figure 3. Chemical structures found in oligoAA and oligo(AA-*b*-Sty) samples. Top is the branched structure of oligoAA. Middle is the chemical structure of the V-501 initiator used to synthesize the samples. Bottom is the linear chemical structure found for the oligo(AA-*b*-Sty) samples synthesized in this work which have a short AA block. The numbers are used to identify signals in the following NMR spectra.

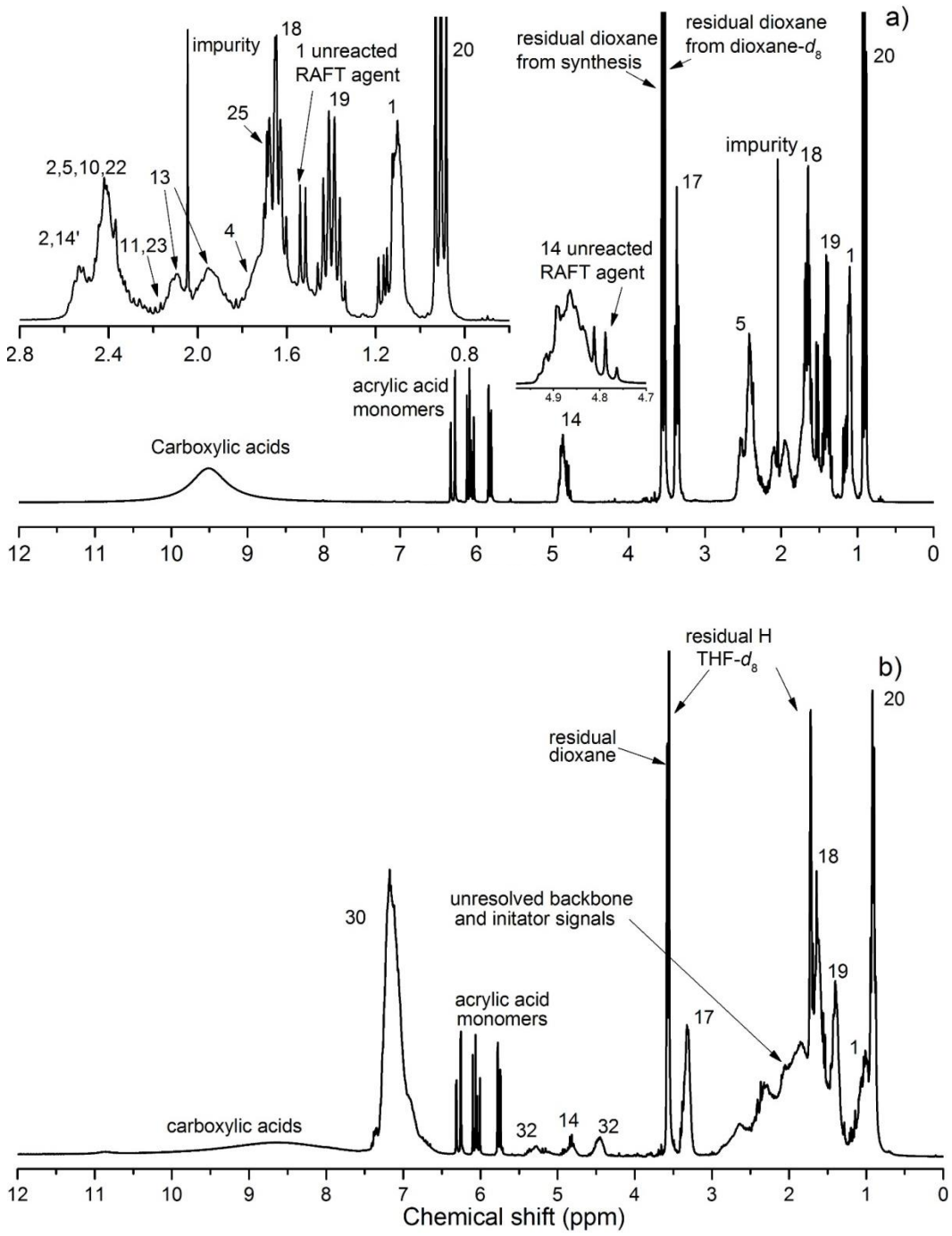

Figure 4. ^{1}H NMR spectra of a) AA4 dissolved in dioxane-d_8 and b) AA4Sty3 dissolved in THF-d_8. The inserts in a) show the backbone region and end group signals. Numbers indicate the nuclei in the corresponding chemical structure shown in Figure 3. The ‘ indicates that it is referring to the second monomer unit from the RAFT agent end group.

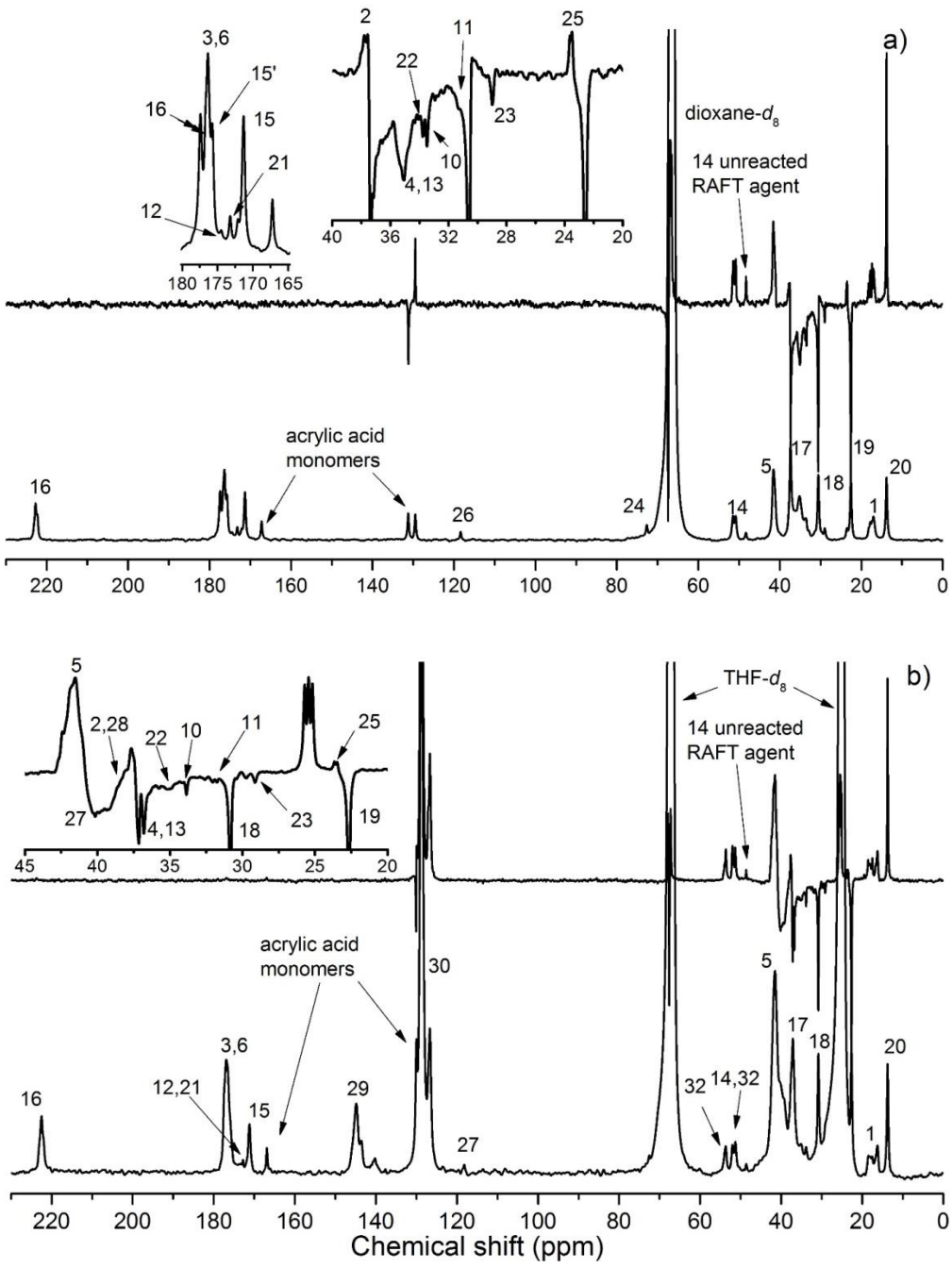

Figure 5. ^{13}C NMR spectra of a) AA4 dissolved in dioxane-d_8 and b) AA4Sty3 dissolved in THF-d_8. Top spectra show the DEPT-135 spectrum while the bottom spectra are quantitative ^{13}C spectra. Numbers indicate the nuclei in the corresponding chemical structure shown in Figure 3. The ‘ indicates that it is referring to the second monomer unit from the H terminated end group.

3.5. DETERMINATION OF AVERAGE CHAIN LENGTH AND DEGREE OF BRANCHING BY NMR SPECTROSCOPY

OligoAA are commonly analyzed by ^{1}H NMR spectroscopy to obtain the average chain length (DP_n). However, from free solution CE it is observed that some samples have a significant fraction of oligomer chains that do not contain a RAFT agent end group. Thus, assuming all chains have a RAFT agent end group results in an overestimation in the DP_n. Furthermore signals from initiators, solvents and other impurities overlapping with the backbone signals can lead to overestimations, although in many cases such signals can be subtracted mitigating the error. The typical DP_n value determined by ^{1}H NMR spectroscopy is assuming that all chains are living. Using free solution CE the weight fraction of dead chains, those without a RAFT agent end group, can be measured. Using this NMR values can be corrected to allow the determination of the DP_n of the chains with a RAFT end group (living chains) but not the DP_n of the whole sample. From ^{13}C NMR spectroscopy it is possible to determine the DP_n assuming all chains have a RAFT agent or H end group which is a far more accurate representation of the sample. However, ^{13}C NMR typically does have error produced from a poor signal-to-noise ratio (*SNR*) and integration. To ensure the *SNR* from the end groups signals of oligoAA below a DP_n of 21 is precise enough for quantification (Relative Standard Deviation, *RSD* <3 %) it was observed that a day long measurement was required. Integration error is caused by the data processing of the spectrum, the setting of baselines, not fully resolved peaks and defining the integration limit. For RAFT agent end group signals the integration error is negligible because they are baseline resolved from any other signals in the ^{13}C NMR spectra, however, the H terminated signals are not as clearly resolved as shown in Figure 6. To estimate the integration error the spectrum of AA21 was processed by 4 independent operators and the *RSD*s of the peak areas were used to

represent the integration error. The *RSD* was found to be 7.0 % for GN11 and 12.0 % for GN10 (GN10 and GN11 refer the group number of the parts of the molecule shown in Figure 3). The estimation is likely an overestimation as the *RSD* on determining the peak areas is also influenced by the Signal-Noise Ratio (*SNR*) and this error is already taken into account by using Equation S-9. Thus a very accurate DP_n of oligoAA can be determined by ^{13}C NMR spectroscopy, such accuracy may be required in applications which are influenced by small variations in chain length such as in gene delivery agents [66, 67].

Obtaining this accurate DP_n is quite a lengthy process and may not be practical in most situations therefore using AA4 as an example the difference in using alternative approaches to determine it are examined, with other comparisons shown in Table 1. The CH of the backbone next to the RAFT end group (GN14) appears at 4.70-4.95 ppm (Figure 4a). This was the signal with the least potential for overlap with other signals that corresponds to the end of the oligomer chain, thus giving almost no integration error and the error from *SNR* is estimated to be <0.6 % giving a very precise DP_n. The DP_n not subtracting overlapping initiator signals for AA4 by ^{1}H NMR spectroscopy was 4.85 ± 0.03 (Equation S-11), after subtracting the initiator signals it was 4.62 ± 0.03 (Equation S-12). The equivalent DP_n by ^{13}C NMR spectroscopy for which all chains are assumed to be living was 4.64 ± 0.04 (Equation S-15). When the all chains are assumed to have RAFT agent or H terminated end groups the DP_n from ^{13}C NMR was 3.70 ± 0.40 (Equation S-16 and S-17). This average value is more similar to the weight distribution found from free solution CE which shows that majority of the chains (~60 % w/w) have a chain length shorter than 4 units (Table 3). The DP_n of the living chains in the sample was found to be 3.36 ± 0.03. Therefore there is no significant difference between the DP_n of the sample assuming all chains are living or

have an H terminated end group, and that of the living chains in the sample. Hence when a ^{13}C NMR spectrum with sufficient sensitivity cannot be produced using ^{1}H NMR and free solution CE to determine the DP_n of the living chains in the sample could be a faster alternative.

When branching is present in PAA a quaternary carbon is produced which can be detected by ^{13}C NMR. The quaternary carbon signal was detected in AA9, AA10, AA21 and confirmed by DEPT experiments to be a quaternary carbon signal (labelled 8 on Figure 6, see also Figures S-22 to S-24). The branching was then quantified in terms of the *DB*, which was calculated as shown in Equations (1) and (2). The *DB* was between 1.0 and 2.8 % which is similar to values reported for PAA synthesized by RAFT (estimates ranging from 0 to 1.9 %) [23] but less than for PAA samples synthesized by Nitroxide Mediated Polymerization (NMP) [22] demonstrating that radical polymerization of acrylic acid will almost always produce significant amounts of branching in the produced oligomers or polymers. For the samples with 4 units or less in chain length the unreacted RAFT agent produces a signal very close to the signal which is produced at the branching point. The unreacted RAFT agent is in much lower quantities in the higher molar mass samples and so does not overlay with the branching signal. The peak area between 46 and 48 ppm in the ^{13}C NMR spectrum of AA4 should correspond to the branching signal, the unreacted RAFT agent and a signal corresponding to the living chains. If this peak area was significantly higher than the peak area of a signal corresponding to living chains and unreacted RAFT agent then branching could be detected. However, no significant difference could be detected thus no measureable amount of branching appears to exist in oligoAA below an average DP_n of 4. To remove the unreacted RAFT agent to detect the branching signal one oligoAA sample was subjected to aminolysis using a procedure described previously [68]. ^{1}H NMR shows

the removal of the RAFT agent (Figure S-25). No branching signal was detected even after the removal of the RAFT agent (Figure S-26).

$$DB\ (\%) = \frac{branched\ units}{all\ monomer\ units} \times 100 \quad (1)$$

$$DB\ (\%) = \frac{I(\mathrm{GN8}) * 2}{I(25-55\ \mathrm{ppm}) - 2I(\mathrm{GN20}) + I(\mathrm{GN1})} \quad (2)$$

where I(25-55 ppm) is the integral of all signals between 25 and 55 ppm, and I(GNx) is the integral of the signal labelled x on Figure 6.

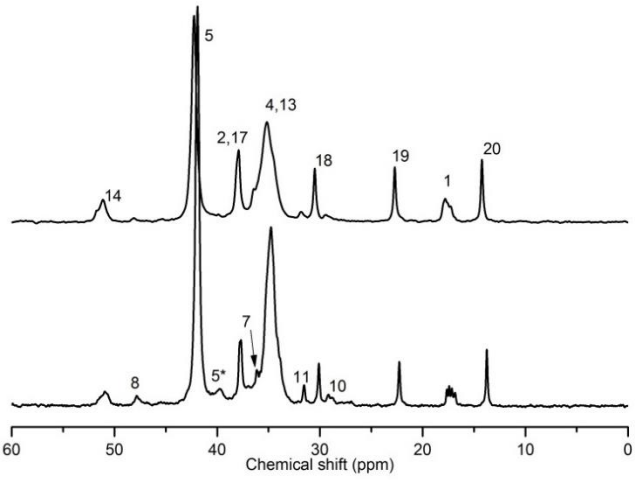

Figure 6. ^{13}C NMR spectra of AA9 (top) and AA21 (bottom) dissolved in D_2O. Only the backbone region is shown as not all the carbonyl signals are quantitative due to an insufficient repetition delay. Numbers indicate the nuclei in the corresponding chemical structure shown in Figure 3. The * indicates the CH adjacent to the branching point.

The source of branching in the oligomers is from intermolecular chain transfer to oligomer or intramolecular transfer to polymer through backbiting. It would be suspected that the low chain length of oligomers would make intermolecular chain transfer unlikely. However, an increase in

580 the *DB* is observed as the chain length increases which suggests the branching maybe linked to
581 intermolecular chain transfer. By comparing the peak areas of GN24 and GN26 in Figure 5a it is
582 estimated that approximately 1 % of the initiator decomposes under these reaction conditions. A
583 larger fraction of dead chains is observed than what would be produced from initiator derived
584 chains. The source of these dead chains could be from transfer to dioxane[22] or potentially from
585 transfer to polymer. In polyacrylates backbiting is suspected to be the predominate source of
586 branching [24, 69-71]. If backbiting was the only source of branching in oligoAA then the
587 amount of dead chains and the effect of chain length is unlikely to be observed [33]. In
588 simulations the possibility for backbiting is taken at 3 monomer units as this is when a 1,5
589 backbiting reaction can occur, which is predicted to be the most favorable backbiting reaction,
590 that can take place to produce a mid-chain radical [72]. Thus when taken to high conversions
591 (>90 %) the same amount of backbiting should be observed for all oligomer chains with greater
592 than 3 monomer units [73]. For samples AA9 and AA21 the fraction of chains with 3 or less
593 monomer units was less than 16 % w/w for both samples (Table 3). Since the fraction is similar
594 for both samples the fraction of chains unable to undergo backbiting is unlikely to be a reason for
595 the differences in *DB* between AA9 and AA21. However in the case of the oligoAAs shorter
596 than AA9 a significantly larger fraction of chains have 3 or less monomer units. The lower chain
597 length oligomers may prevent both intra and intermolecular (chain) transfer to polymer and
598 produce no detectable amount of branching. Thus it is likely that both intra and intermolecular
599 (chain) transfer to polymer take place in formation of branches in oligomers with one not being
600 more likely to occur than the other.
601
602

3.6. DISTRIBUTION OF MOLAR MASSES OF OLIGOAA

Although it is possible to obtain a highly accurate DP_n of oligoAA by ^{13}C NMR it is only an average value for the sample. Using free solution CE the distribution of molar masses of the smaller molar mass chains can be determined. The partial weight distribution of molar masses for the oligoAA are shown in Table 3. The weight distribution of molar masses is of particular importance in ensuring oligoAA samples have similar chain lengths as even though the average maybe the same the distributions may differ. The weight distribution of molar masses of the oligoAA is of particular importance in the production of self-assembled structures when oligoAA are chain extended with a hydrophobic monomer. This is because the low molar mass oligoAA chains with only 1 to 3 hydrophilic monomer units may significantly alter the phase behavior. Using free solution CE the low molar mass oligoAA chains can be quantified and chains with 3 or less AA units were found in all oligoAA even with average chain lengths of 21.

The weight fractions of dead chains in the oligoAA samples were also determined by free solution CE, double UV detection at 200 and 290 nm to identify the peaks (see Figure S-4 and supporting information section 4.1). The weight fraction would be slightly underestimated as the living chains would absorb UV at 200 nm more than the dead chains due to additional absorption from the RAFT agent end group. The underestimation from assuming all the absorbance is a result of only one functional group, the carbonyl in the case of oligoAA, in an oligomer sample is suspected to be less than 10 % [74]. It should be noted that such errors are present in all separation methods for oligoAA as the RAFT agent end group changes the dn/dc (refractive index detection) and the ionization efficiency which would influence SEC and ESI-MS

measurements respectively. Nevertheless knowing the amount of dead chains is crucial when making block copolymers as the dead chains will be present as impurities in the final product.

3.7. PURITY OF OLIGOAA AND OLIGO(AA-*b*-STY)

Measuring the purity of oligomers and their block co-oligomers is highly important because few purification methods are available to purify them. Purification techniques generally applied to polymers result in loss of the oligomer fraction as well. The alternative to purifying the oligomer sample is to conduct the synthesis with little unreacted material or side products. To adapt the synthesis methods to measure the impurities are required. Using free solution CE the amount of unreacted RAFT agent could be determined in all oligoAA and block co-oligomer samples. Furthermore the conversion of the RAFT agent can also be measured to very small concentrations. The Limit of Detection (LOD, when *SNR* is 3) for the RAFT agent was estimated to be 26 mg L^{-1} and the Limit of Quantification (LOQ, when *SNR* is 10) was 88 mg L^{-1}. It was observed that full conversion of the RAFT agent was obtained in oligoAA samples with a DP_n greater than 10 and with 9 units >99 % of the RAFT agent reacted. Conversion of the RAFT agent can also be measured by NMR spectroscopy; however, the RAFT agent signal suffers from integration error and the signal cannot be detected in samples with a chain length of 6 or greater due to the broadening of the backbone signals.

The purity in terms of the presence of homo-oligomers in block co-oligomers is important in understanding their phase behavior. OligoAA can be present in block co-oligomers due to the presence of dead chains as well as chains with a RAFT agent end group that were not reinitiated. Furthermore residual initiator can decompose to react with the new monomer to produce a homo-

oligomer. For block copolymers these homopolymers and dead chains are almost always detected [44, 75]. Dead oligoAA chains were detected in all samples by free solution CE, demonstrating that their formation in the synthesis of the oligoAA block will cause them to be present in the block co-oligomer. The fraction of dead oligoAA chains is generally considered to be very low. ESI-MS has previously been used to detect dead chains in oligomers and they were found to be in low quantities, while free solution CE found that dead chains constituted at least 13 % w/w of the oligoAA samples [13]. ESI-MS, with the specific conditions used in this literature may underestimate the amount of dead chains as the RAFT agent end group may enhance the ionization relative to the chains without a RAFT agent, artificially making it appear that there are less dead chains. Similar but different ESI-MS conditions show that direct infusion of the RAFT agent was leading to a strong underestimate of the amount of unreacted RAFT agent [18]. Therefore free solution CE provides a better method for quantifying the amount of dead chains in oligoAA and the block co-oligomers.

Using ^{13}C NMR the percentage of chains with H terminated chains to living chains can be determined. Within the sensitivity of the ^{13}C NMR measurement a significant amount of H terminated chains were detected in AA4 and AA9. However, in AA21 the H terminated signal was not significantly larger than the branching signal. When a branch is formed an H terminated end is produced as well. The source of these H terminated end groups could be from transfer to solvent as the amount of initiator derived chains is very low due to the minimal decomposition of the initiator as described earlier. The percentage of H terminated end groups was (20.4 ± 3.2) % and (3.2 ± 0.5) % for AA4 and AA9 respectively. The decreasing percentage of H ends with increasing chain length is in agreement the weight percentage of dead chains found by free

671 solution CE shown in Table 3. However, the difference in the weight percentage of dead chains
672 and the difference in H terminated chains between AA4 and AA9 is not in agreement.
673 Furthermore AA21 has a similar weight percentage of dead chains to AA9 but a far lower
674 percentage of H terminated end groups. When branching is produced by intermolecular chain
675 transfer to polymer a dead chain forms with an H end group while the end of the branch would
676 possess a RAFT agent moiety. Therefore when subtracting the branching quaternary carbon
677 integral from the H end group NMR integral, the resulting H end group cannot be distinguished
678 from H signals corresponding to branch ends, preventing the detection of these dead chains. Thus
679 free solution CE would detect dead chains formed from intermolecular chain transfer to polymer
680 while NMR would not. This may explain why significant higher weight percentages of dead
681 chains are detected in the longer chain length oligomers but a little to no H terminated chain ends
682 were detected by NMR. This further suggests that intermolecular chain transfer to polymer is
683 significantly contributing the branching of oligoAA.
684
685 3.8. CHEMICAL HETEROGENEITY
686 The separation of oligo(AA-*b*-Sty) by free solution CE, using the conditions recommended for
687 high resolution, identifies many different chemical structures present in the samples (Figure 7).
688 There is a decrease in the weight-average electrophoretic mobility (μ_w) of the block co-oligomers
689 with respect to oligoAA from 4.46×10^{-8} to 4.38×10^{-8} $m^2V^{-1}s^{-1}$ with the addition of 1 Sty unit
690 on average. The weight average electrophoretic mobility further decreases as the Sty content
691 increases. The decrease in electrophoretic mobility is because the Sty block adds hydrodynamic
692 friction to the chains without adding any additional charge. A molecule's electrophoretic

693 mobility is dependent on the molar mass, composition, end group and tacticity of the block co-
694 oligomer chains, thus yielding very complex separations.
695
696 The PABTC RAFT agent (1R) and the dead chains are detected in all 3 oligo(AA-*b*-Sty)
697 samples. For AA4Sty1 chains corresponding to 2 and 3 AA units with a RAFT end group were
698 still detected but no longer for AA4Sty2. The higher molar mass oligoAA chains are no longer
699 present in AA4Sty3 while the some RAFT agent is remaining, indicating that the macroRAFT
700 agent is more reactive than the PABTC RAFT agent. Nevertheless Sty has added to the
701 remaining RAFT agent, giving a peak at 2.0×10^{-8} $m^2V^{-1}s^{-1}$, which is a lower electrophoretic
702 mobility than that of the RAFT agent. The number of Sty units added is unknown but it is likely
703 1 or 2 units as a higher Sty content would not be soluble in the aqueous solvent.
704
705 The blocking efficiency is the fraction of living homo-oligomers reinitiated. It can be measured
706 by ^{1}H NMR in a non-aqueous solvent, as the Sty units give different chemical shifts to AA units
707 next the RAFT agent end group. Aqueous solvents give a solvent signal which overlaps with the
708 signals adjacent to the RAFT agent end group. The blocking efficiency when 3 units of Sty were
709 added was 73.2 %, meaning that over a quarter of the oligoAA chains with RAFT agent end
710 groups have not been reinitiated. With the addition of 1 Sty unit over half the living chains were
711 reinitiated (Table 1). From free solution CE the electrophoretic mobility of AA4Sty3 has almost
712 completely shifted below 4.75×10^{-8} $m^2V^{-1}s^{-1}$ which is where the chains with greater than 4 AA
713 units are present, indicating that the majority of these chains have been reinitiated. A significant
714 amount of RAFT agent is present in AA4Sty3 which would contribute to the unreacted oligoAA
715 homopolymer along with other oligoAA chains of 2 or 3 AA units in length which are in too

716 small a quantity to be detected by free solution CE amongst the block co-oligomer chains.
717 Therefore knowing the fraction of small chain oligoAA in a sample is important as they are the
718 least likely chains to be extended and can result in additional residual homo-oligomers in the
719 block co-oligomer sample. The presence of these homopolymers may play a role in surface
720 activity[8] and thus colloid formation.

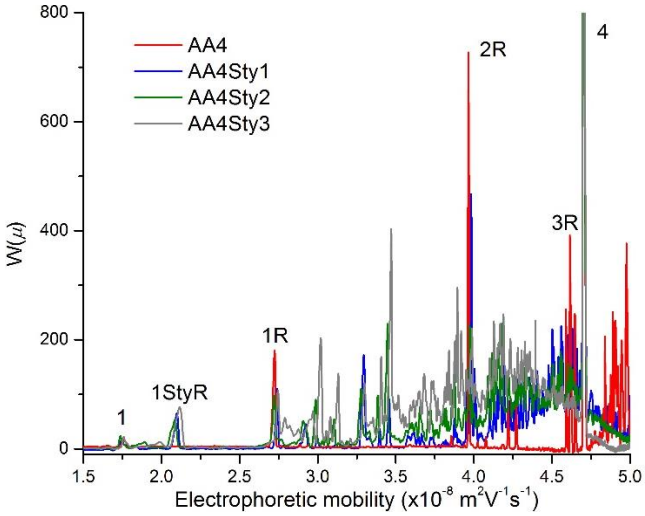

721

722 Figure 7. Separation of oligo(AA-*b*-Sty) and their oligoAA precursor by free solution CE. The
723 number indicates the number of AA units, R represents a RAFT agent end group. 1StyR is 1 AA
724 unit with Sty units and a RAFT agent end group. Separations occurred with a 400 mM sodium
725 borate buffer as the BGE, 59.2 cm total length capillary, 50.7 cm effective length, injection
726 concentration 5 g L^{-1}. Separations took place at 25 °C and 30 kV, detection at 200 nm.

727

728 The dispersity of the electrophoretic mobility distribution represents the heterogeneity in a
729 sample and has previously been used to describe the heterogeneity in branching architectures for
730 charged homopolymers and composition for copolymers [39, 43]. Although the block co-
731 oligomers are separated according to a number of molecular parameters the dispersity can be
732 used to describe the heterogeneity at which the polymerization is occurring. If Sty monomers

were adding to each chain equally then the dispersity of the distribution of electrophoretic mobilities would remain the same. There is a noticeable increase in the dispersity from AA4Sty1 to AA4Sty2 showing that the heterogeneity increased but when more Sty is added to make AA4Sty3 the dispersity is experimentally the same. These findings are in agreement with the penultimate model rather than the terminal model for propagating radicals of Sty and AA, which has been discussed in the literature previously [76]. When an average 2 Sty units are present the propagation of Sty units is added less heterogeneously, although additional chain lengths of Sty were not examined in this study. This suggests that the Sty monomers may preferentially add to particular chains and then equally between all chains. This would then mean there are changes in the heterogeneity of the molar mass and composition distributions of the different block co-oligomers. To further improve the characterization of the oligo(AA-*b*-Sty) MS detection could be used to identify the exact molecular structure corresponding to each peak.

Table 3. Partial weight distribution of molar mass oligoAA and oligo(AA-*b*-Sty) samples expressed as %(w/w) of each species (the number in the first column indicates the number of AA units and R indicates the presence of RAFT end group as shown in Figure 1). The blocking efficiency, the weight-average electrophoretic mobility (μ_w) and the dispersity of the electrophoretic mobility distribution $D(1,0)$ are also listed.

Sample	AA21 n=6	AA9 n=6	AA4 n=3	AA4-Sty1 n=2	AA4-Sty2 n=2	AA4-Sty3 n=2
1	0.45 ± 0.04	1.20 ± 0.06	0.12 ± 0.03	0.69 ± 0.08	0.60 ± 0.16	0.41 ± 0.05
1R	<LOD[a]	0.28 ± 0.01	7.47 ± 0.68	2.09 ± 0.03	2.45 ± 0.01	1.43 ± 0.26

2	0.50 ± 0.02	0.57 ± 0.03	0.37 ± 0.05	NR[c]	NR	NR
2R	0.11 ± 0.01	0.83 ± 0.06	13.57 ± 0.73	4.36 ± 0.33	NR	NR
3	14.63 ± 0.70	11.83 ± 0.44	2.24 ± 0.25	NR	NR	NR
3R	NR	0.38 ± 0.11	13.25 ± 1.08	NR	NR	NR
4	NR	NR	24.93 ± 2.42	20.57 ± 1.13	9.54 ± 5.83	8.91 ± 3.67
≥3	98.95 ± 0.05	97.13 ± 0.15	78.48 ± 1.23 [38.07 ± 4.04[b]]	NR	NR	NR
StyR	-	-	-	1.89 ± 0.15	2.11 ± 0.73	2.22 ± 0.38
Dead chains	15.58	13.60	27.65	21.26	10.14	9.32
Fraction of block copolymer	-	-	-	≥ 56.4	≥ 77.7	≥ 80.6
μ_w (m^2 V^{-1} s^{-1})	4.88×10^{-8}	5.03×10^{-8}	4.46×10^{-8}	4.38×10^{-8}	4.15×10^{-8}	3.99×10^{-8}
$D(1,0)$	-	-	-	1.013	1.023	1.021

[a]LOD stands for Limit of Detection [b](% w/w) of chains ≥AA3R [c]NR stands for not resolved

4. CONCLUSIONS

OligoAA and their block co-oligomers have many applications which require detailed knowledge of their chemical structure in order to properly tailor their properties. Even when

improving the SEC resolution free solution CE methods have been shown to give more information about the distribution of end groups and molar masses. Furthermore different CE conditions can be used depending on the desired information. Monitoring the conversion of RAFT agent can be performed with separations shorter than 4 min. In contrast high resolution separations can be achieved with peak capacities greater than 400 which is 10 times greater than what has been achieved for LC of oligoSty. The high resolution separation from free solution CE was applied to oligo(AA-*b*-Sty) providing information regarding the homogeneity of the chemical structures present in terms of their distribution of end groups, chemical composition and molar mass. The only other quantitative separation technique which may be able to provide similar resolution for oligoAA is ion chromatography which has been used to assess the molar mass distribution of oligophosphates [77]. Alternatively to improve to further improve the peak capacity of free solution CE a two dimensional approach using both ion chromatography and free solution CE could be used. From the use of 1D and 2D NMR spectra a near complete assignment of all the ^{1}H and ^{13}C NMR signals was shown. Thus very accurate molar masses of oligomers were obtained using appropriate NMR conditions (such as solvent and temperature) to obtain the average value while CE can give insight into the molar mass distribution. The in-depth characterization of these materials is shown through the combination of these two techniques and the importance of these results are highlighted in this work through the use of as all samples were shown to differ from the targeted synthesis.

Oligomers are often assumed to be linear however the ^{13}C NMR experiments conducted in this work reveal that oligoAA with average chain lengths of 9 units (8 added units and 1 from RAFT agent) have a detectable degree of branching. This branching could also be present in other

779 oligomers and shows that the assumption that oligomers do not contain branching is invalid.
780 Hence a comprehensive characterization of the chemical structure of oligoAA and oligo(AA-*b*-
781 Sty) was achieved using free solution CE and NMR spectroscopy. The majority of the
782 characterization methods shown here could be routinely applied to oligoAA and other
783 oligoelectrolytes.
784
785 ACKNOWLEDGMENTS
786 This work was supported by the Australian Research Council's Discovery funding scheme
787 (DP130101471). We thank Dr Yohann Guillaneuf (Aix-Marseille University) and Elham
788 Hosseini Nejad for the synthesis of some of the oligomers and for discussion. We are grateful to
789 Martina Adler (PSS, Mainz, Germany) for suggesting using trifluoroacetic acid as additive for
790 THF SEC. We thank Alison Maniego, Joel Thevarajah and Andrew Nettleton for assistance with
791 NMR experiments. AS acknowledges the Australian Commonwealth government for an RTP
792 scholarship.
793
794 REFERENCES
795 [1] R.Q. Song, H. Cölfen, Additive controlled crystallization, Crystengcomm, 13 (2011) 1249-
796 1276.
797 [2] B. Bae, T. Hoshi, K. Miyatake, M. Watanabe, Sulfonated block poly(arylene ether sulfone)
798 membranes for fuel cell applications via oligomeric sulfonation, Macromolecules, 44 (2011)
799 3884-3892.
800 [3] J.S. Hyslop, L.M.G. Hall, A.A. Umansky, C.P. Palmer, RAFT polymerized nanoparticles:
801 Influences of shell and core chemistries on performance for electrokinetic chromatography,
802 Electrophoresis, 35 (2014) 728-735.
803 [4] C.P. Palmer, E.F. Hilder, J.P. Quirino, P.R. Haddad, Electrokinetic chromatography and mass
804 spectrometric detection using latex nanoparticles as a pseudostationary phase, Anal. Chem., 82
805 (2010) 4046-4054.
806 [5] B.T.T. Pham, C.H. Such, B.S. Hawkett, Synthesis of polymeric janus nanoparticles and their
807 application in surfactant-free emulsion polymerizations, Poly. Chem., 6 (2015) 426-435.

[6] A. Khodabandeh, R. Dario Arrua, C.T. Desire, T. Rodemann, S.A.F. Bon, S.C. Thickett, E.F. Hilder, Preparation of inverse polymerized high internal phase emulsions using an amphiphilic macro-RAFT agent as sole stabilizer, Poly. Chem., 7 (2016) 1803-1812.
[7] V.T. Huynh, D. Nguyen, C.H. Such, B.S. Hawkett, Polymer Coating of Graphene Oxide via Reversible Addition-Fragmentation Chain Transfer Mediated Emulsion Polymerization, J. Polym. Sci., Part A: Polym. Chem., 53 (2015) 1413-1421.
[8] D.E. Ganeva, E. Sprong, H. De Bruyn, G.G. Warr, C.H. Such, B.S. Hawkett, Particle formation in ab initio RAFT mediated emulsion polymerization systems, Macromolecules, 40 (2007) 6181-6189.
[9] C.H. Such, E. Rizzardo, A.K. Serelis, B.S. Hawkett, R.G. Gilbert, C.J. Ferguson, R.J. Hughes, Aqueous dispersions of polymer particles, University of Sydney, Australia . 2003, pp. 90 pp.
[10] D. Nguyen, H.S. Zondanos, J.M. Farrugia, A.K. Serelis, C.H. Such, B.S. Hawkett, Pigment encapsulation by emulsion polymerization using macro-RAFT copolymers, Langmuir, 24 (2008) 2140-2150.
[11] M. Siauw, B.S. Hawkett, S. Perrier, Short chain amphiphilic diblock co-oligomers via RAFT polymerization, J. Polym. Sci., Part A: Polym. Chem., 50 (2012) 187-198.
[12] M. Gaborieau, P. Castignolles, Size-exclusion chromatography (SEC) of branched polymers and polysaccharides, Anal. Bioanal Chem., 399 (2011) 1413-1423.
[13] J.M. Heinen, A.C.M. Blom, B.S. Hawkett, G.G. Warr, Phase behavior of amphiphilic diblock co-oligomers with nonionic and ionic hydrophilic groups, J. Phys. Chem. B, 117 (2013) 3005-3018.
[14] M. Girod, T.N.T. Phan, L. Charles, Microstructural Study of a Nitroxide-Mediated Poly(Ethylene Oxide)/Polystyrene Block Copolymer (PEO-*b*-PS) by Electrospray Tandem Mass Spectrometry, J. Am. Soc. Mass Spectrom., 19 (2008) 1163-1175.
[15] J.A. Leenheer, C.E. Rostad, P.M. Gates, E.T. Furlong, I. Ferrer, Molecular resolution and fragmentation of fulvic acid by electrospray ionization/multistage tandem mass spectrometry, Anal. Chem., 73 (2001) 1461-1471.
[16] M.W.F. Nielen, Characterization of synthetic polymers by size-exclusion chromatography/electrospray ionization mass spectrometry, Rapid Commun. Mass Spectrom., 10 (1996) 1652-1660.
[17] C.M. Guttman, K.M. Flynn, W.E. Wallace, A.J. Kearsley, Quantitative mass spectrometry and polydisperse materials: Creation of an absolute molecular mass distribution polymer standard, Macromolecules, 42 (2009) 1695-1702.
[18] M. Gaborieau, T.J. Causon, Y. Guillaneuf, E.F. Hilder, P. Castignolles, Molecular weight and tacticity of oligoacrylates by capillary electrophoresis-mass spectrometry, Aust. J. Chem., 63 (2010) 1219-1226.
[19] M. Girod, T.N.T. Phan, L. Charles, Tuning block copolymer structural information by adjusting salt concentration in liquid chromatography at critical conditions coupled with electrospray tandem mass spectrometry, Rapid Commun. Mass Spectrom., 23 (2009) 1476-1482.
[20] J.S.K. Leswin, Particle Formation in RAFT-mediated Emulsion Polymerization, Science. School of Chemistry. Key Centre for Polymer Colloids, PhD Thesis, University of Sydney, Sydney, 2007. http://hdl.handle.net/2123/2176
[21] A.R. Maniego, D. Ang, Y. Guillaneuf, C. Lefay, D. Gigmes, J.R. Aldrich-Wright, M. Gaborieau, P. Castignolles, Separation of poly(acrylic acid) salts according to topology using capillary electrophoresis in the critical conditions, Anal. Bioanal Chem., 405 (2013) 9009-9020.

[22] L. Couvreur, C. Lefay, J. Belleney, B. Charleux, O. Guerret, S. Magnet, First Nitroxide-Mediated Controlled Free-Radical Polymerization of Acrylic Acid, Macromolecules, 36 (2003) 8260-8267.
[23] J. Loiseau, N. Doërr, J.M. Suau, J.B. Egraz, M.F. Llauro, C. Ladavière, J. Claverie, Synthesis and Characterization of Poly(acrylic acid) Produced by RAFT Polymerization. Application as a Very Efficient Dispersant of $CaCO_3$, Kaolin, and TiO_2, Macromolecules, 36 (2003) 3066-3077.
[24] N.F.G. Wittenberg, C. Preusser, H. Kattner, M. Stach, I. Lacík, R.A. Hutchinson, M. Buback, Modeling Acrylic Acid Radical Polymerization in Aqueous Solution, Macromol. React. Eng., (2015).
[25] J.B. Lena, A.K. Goroncy, J.J. Thevarajah, A.R. Maniego, G.T. Russell, P. Castignolles, M. Gaborieau, Effect of transfer agent, temperature and initial monomer concentration on branching in poly(acrylic acid): A study by13C NMR spectroscopy and capillary electrophoresis, Polymer, 114 (2017) 209-220.
[26] N.M. Ahmad, B. Charleux, C. Farcet, C.J. Ferguson, S.G. Gaynor, B.S. Hawkett, F. Heatley, B. Klumperman, D. Konkolewicz, P.A. Lovell, K. Matyjaszewski, R. Venkatesh, Chain transfer to polymer and branching in controlled radical polymerizations of n-butyl acrylate, Macromol. Rapid Commun., 30 (2009) 2002-2021.
[27] P. Castignolles, R. Graf, M. Parkinson, M. Wilhelm, M. Gaborieau, Detection and quantification of branching in polyacrylates by size-exclusion chromatography (SEC) and melt-state 13C NMR spectroscopy, Polymer, 50 (2009) 2373-2383.
[28] M. Gaborieau, S.P.S. Koo, P. Castignolles, T. Junkers, C. Barner-Kowollik, Reducing the degree of branching in polyacrylates via midchain radical patching: A quantitative melt-state NMR study, Macromolecules, 43 (2010) 5492-5495.
[29] B. Wenn, G. Reekmans, P. Adriaensens, T. Junkers, Photoinduced acrylate polymerization: Unexpected reduction in chain branching, Macromol. Rapid Commun., 36 (2015) 1479-1485.
[30] D. Konkolewicz, H. De Bruyn, B.S. Hawkett, Effect of stabilizer functionality on the kinetics of emulsion polymerization in hairy particles, Macromolecules, 44 (2011) 8744-8754.
[31] I. Lacík, M. Stach, P. Kasák, V. Semak, L. Uhelská, A. Chovancová, G. Reinhold, P. Kilz, G. Delaittre, B. Charleux, I. Chaduc, F. D'Agosto, M. Lansalot, M. Gaborieau, P. Castignolles, R.G. Gilbert, Z. Szablan, C. Barner-Kowollik, P. Hesse, M. Buback, SEC Analysis of Poly(Acrylic Acid) and Poly(Methacrylic Acid), Macromol. Chem. Phys., 216 (2015) 23-37.
[32] A.R. Maniego, A.T. Sutton, M. Gaborieau, P. Castignolles, Assessment of the branching quantification in poly(acrylic acid): is it as easy as it seems?, Macromolecules, (2017) 9032-9041.
[33] D. Konkolewicz, S. Sosnowski, D.R. D'Hooge, R. Szymanski, M.F. Reyniers, G.B. Marin, K. Matyjaszewski, Origin of the difference between branching in acrylates polymerization under controlled and free radical conditions: A computational study of competitive processes, Macromolecules, 44 (2011) 8361-8373.
[34] Y. Reyes, J.M. Asua, Revisiting chain transfer to polymer and branching in controlled radical polymerization of butyl acrylate, Macromol. Rapid Commun., 32 (2011) 63-67.
[35] T. Junkers, C. Barner-Kowollik, The role of mid-chain radicals in acrylate free radical polymerization: Branching and scission, J. Polym. Sci., Part A: Polym. Chem., 46 (2008) 7585-7605.

[36] C.J. Ferguson, R.J. Hughes, D. Nguyen, B.T.T. Pham, R.G. Gilbert, A.K. Serelis, C.H. Such, B.S. Hawkett, Ab initio emulsion polymerization by RAFT-controlled self-assembly, Macromolecules, 38 (2005) 2191-2204.
[37] J.D. Oliver, M. Gaborieau, E.F. Hilder, P. Castignolles, Simple and robust determination of monosaccharides in plant fibers in complex mixtures by capillary electrophoresis and high performance liquid chromatography, J. Chromatogr. A, 1291 (2013) 179-186.
[38] J.J. Thevarajah, M. Gaborieau, P. Castignolles, Separation and characterization of synthetic and natural complex polymers with capillary electrophoresis, Adv. Chem., 2014 (2014) 11.
[39] J.J. Thevarajah, A.T. Sutton, A.R. Maniego, E.G. Whitty, S. Harrisson, H. Cottet, P. Castignolles, M. Gaborieau, Quantifying the heterogeneity of chemical structures in complex charged polymers through the dispersity of their distributions of electrophoretic mobilities or of compositions, Anal. Chem., 88 (2016) 1674-1681.
[40] H. Cottet, P. Gareil, Separation of synthetic (Co)polymers by capillary electrophoresis techniques, Methods Mol. Biol. (Totowa, NJ, U. S.): Capillary Electrophoresis, Humana Press Inc.2008, pp. 541-567.
[41] D.L. Taylor, C.J. Ferris, A.R. Maniego, P. Castignolles, M. in het Panhuis, M. Gaborieau, Characterization of Gellan Gum by Capillary Electrophoresis, Aust. J. Chem., 65 (2012) 1156-1164.
[42] M. Mnatsakanyan, J.J. Thevarajah, R.S. Roi, A. Lauto, M. Gaborieau, P. Castignolles, Separation of chitosan by degree of acetylation using simple free solution capillary electrophoresis, Anal. Bioanal Chem., 405 (2013) 6873-6877.
[43] J.J. Thevarajah, M.P. Van Leeuwen, H. Cottet, P. Castignolles, M. Gaborieau, Determination of the distributions of degrees of acetylation of chitosan, Int. J. Biol. Macromol., 95 (2017) 40-48.
[44] A.T. Sutton, E. Read, A.R. Maniego, J.J. Thevarajah, J.D. Marty, M. Destarac, M. Gaborieau, P. Castignolles, Purity of double hydrophilic block copolymers revealed by capillary electrophoresis in the critical conditions, J. Chromatogr. A, 1372 (2014) 187-195.
[45] F. Oukacine, S. Bernard, I. Bobe, H. Cottet, Physico-chemical characterization of polymeric micelles loaded with platinum derivatives by capillary electrophoresis and related methods, J. Controlled Release, 196 (2014) 139-145.
[46] J. Reboul, T. Nugay, N. Anik, H. Cottet, V. Ponsinet, M. In, P. Lacroix-Desmazes, C. Gerardin, Synthesis of double hydrophilic block copolymers and induced assembly with oligochitosan for the preparation of polyion complex micelles, Soft Matter, 7 (2011) 5836-5846.
[47] U. Pyell, A.H. Jalil, D.A. Urban, C. Pfeiffer, B. Pelaz, W.J. Parak, Characterization of hydrophilic coated gold nanoparticles via capillary electrophoresis and Taylor dispersion analysis. Part II: Determination of the hydrodynamic radius distribution - Comparison with asymmetric flow field-flow fractionation, J. Colloid Interface Sci., 457 (2015) 131-140.
[48] E. Duffy, D.P. Mitev, P.N. Nesterenko, A.A. Kazarian, B. Paull, Separation and characterisation of detonation nanodiamond by capillary zone electrophoresis, Electrophoresis, 35 (2014) 1864-1872.
[49] P. Castignolles, M. Gaborieau, E.F. Hilder, E. Sprang, C.J. Ferguson, R.G. Gilbert, High-resolution separation of oligo(acrylic acid) by capillary zone electrophoresis, Macromol. Rapid Commun., 27 (2006) 42-46.
[50] E. Stellwagen, A. Abdulla, Q. Dong, N.C. Stellwagen, Electrophoretic mobility is a reporter of hairpin structure in single-stranded DNA oligomers, Biochemistry, 46 (2007) 10931-10941.

[51] H. Cottet, P. Gareil, O. Theodoly, C.E. Williams, A semi-empirical approach to the modeling of the electrophoretic mobility in free solution: Application to polystyrenesulfonates of various sulfonation rates, Electrophoresis, 21 (2000) 3529-3540.
[52] N. Ouadah, C. Moire, J.F. Kuntz, F. Brothier, H. Cottet, Analysis and characterization of aluminum chlorohydrate oligocations by capillary electrophoresis, J. Chromatogr. A, 1492 (2017) 144-150.
[53] J. Chamieh, M. Martin, H. Cottet, Quantitative analysis in capillary electrophoresis: Transformation of raw electropherograms into continuous distributions, Anal. Chem., 87 (2015) 1050-1057.
[54] G.R. Fulmer, A.J.M. Miller, N.H. Sherden, H.E. Gottlieb, A. Nudelman, B.M. Stoltz, J.E. Bercaw, K.I. Goldberg, NMR chemical shifts of trace impurities: Common laboratory solvents, organics, and gases in deuterated solvents relevant to the organometallic chemist, Organometallics, 29 (2010) 2176-2179.
[55] M. Adler, H. Pasch, C. Meier, R. Senger, H.G. Koban, M. Augenstein, G. Reinhold, Molar mass characterization of hydrophilic copolymers, 1 Size exclusion chromatography of neutral and anionic (meth)acrylate copolymers, E-Polymers, (2004).
[56] S. Schmitz, A.C. Dona, P. Castignolles, R.G. Gilbert, M. Gaborieau, Assessment of the extent of starch dissolution in dimethyl sulfoxide by ^{1}H NMR spectroscopy, Macromol. Biosci., 9 (2009) 506-514.
[57] J.J. Thevarajah, J.C. Bulanadi, M. Wagner, M. Gaborieau, P. Castignolles, Towards a less biased dissolution of chitosan, Anal. Chim. Acta, 935 (2016) 258-268.
[58] E.G. Whitty, A.R. Maniego, S.A. Bentwitch, Y. Guillaneuf, M.R. Jones, M. Gaborieau, P. Castignolles, Cellular response to linear and branched poly(acrylic acid), Macromol. Biosci., 15 (2015) 1724-1734.
[59] C. De Stefano, A. Gianguzza, D. Piazzese, S. Sammartano, Polyacrylates in aqueous solution. The dependence of protonation on molecular weight, ionic medium and ionic strength, Reactive & Functional Polymers, 55 (2003) 9-20.
[60] M. Rollet, B. Pelletier, A. Altounian, D. Berek, S. Maria, E. Beaudoin, D. Gigmes, Separation of parent homopolymers from polystyrene-b-poly(ethylene oxide)-b-polystyrene triblock copolymers by means of liquid chromatography: 1. Comparison of different methods, Anal. Chem., 86 (2014) 2694-2702.
[61] A. Ibrahim, S.A. Allison, H. Cottet, Extracting information from the ionic strength dependence of electrophoretic mobility by use of the slope plot, Anal. Chem., 84 (2012) 9422-9430.
[62] D.J. Keddie, A guide to the synthesis of block copolymers using reversible-addition fragmentation chain transfer (RAFT) polymerization, Chem. Soc. Rev., 43 (2014) 496-505.
[63] K. Jinno, Y. Han, M. Nakamura, Analysis of anxiolytic drugs by capillary electrophoresis with bare and coated capillaries, J. Capillary Electrophor., 3 (1996) 139-145.
[64] K. Jinno, Y. Han, H. Sawada, Analysis of toxic drugs by capillary electrophoresis using polyacrylamide-coated columns, Electrophoresis, 18 (1997) 284-286.
[65] M.J. Gray, G.R. Dennis, P.J. Slonecker, R.A. Shalliker, Utilising retention correlation for the separation of oligostyrenes by coupled-column liquid chromatography, J. Chromatogr. A, 1073 (2005) 3-9.
[66] M. Furuhata, H. Kawakami, K. Toma, Y. Hattori, Y. Maitani, Design, synthesis and gene delivery efficiency of novel oligo-arginine-linked PEG-lipids: Effect of oligo-arginine length, Int. J. Pharm., 316 (2006) 109-116.

[67] C. Scholz, P. Kos, L. Leclercq, X. Jin, H. Cottet, E. Wagner, Correlation of length of linear oligo(ethanamino) amides with gene transfer and cytotoxicity, ChemMedChem, 9 (2014) 2104-2110.
[68] V. Lima, X. Jiang, J. Brokken-Zijp, P.J. Schoenmakers, B. Klumperman, R. Van Der Linde, Synthesis and characterization of telechelic polymethacrylates via RAFT polymerization, J. Polym. Sci., Part A: Polym. Chem., 43 (2005) 959-973.
[69] P. Derboven, P.H.M. Van Steenberge, J. Vandenbergh, M.-F. Reyniers, T. Junkers, D.R. D'Hooge, G.B. Marin, Improved Livingness and Control over Branching in RAFT Polymerization of Acrylates and the difference made by microflow synthesis, Macromol. Rapid Commun., 36 (2015) 2149-2155.
[70] C. Farcet, J. Belleney, B. Charleux, R. Pirri, Structural characterization of nitroxide-terminated poly(n-butyl acrylate) prepared in bulk and miniemulsion polymerizations, Macromolecules, 35 (2002) 4912-4918.
[71] J.M. Asua, S. Beuermann, M. Buback, P. Castignolles, B. Charleux, R.G. Gilbert, R.A. Hutchinson, J.R. Leiza, A.N. Nikitin, J.P. Vairon, A.M. Van Herk, Critically evaluated rate coefficients for free-radical polymerization, 5: Propagation rate coefficient for butyl acrylate, Macromol. Chem. Phys., 205 (2004) 2151-2160.
[72] D. Cuccato, E. Mavroudakis, M. Dossi, D. Moscatelli, A density functional theory study of secondary reactions in n-butyl acrylate free radical polymerization, Macromol. Theory Simul., 22 (2013) 127-135.
[73] S. Hamzehlou, Y. Reyes, J.R. Leiza, Detailed Microstructure Investigation of Acrylate/Methacrylate Functional Copolymers by Kinetic Monte Carlo Simulation, Macromol. React. Eng., 6 (2012) 319-329.
[74] I. Hintersteiner, T. Schmid, M. Himmelsbach, C.W. Klampfl, W.W. Buchberger, Quantitative analysis of hindered amine light stabilizers by CZE with UV detection and quadrupole TOF mass spectrometric detection, Electrophoresis, 35 (2014) 2965-2971.
[75] D. Berek, Separation of minor macromolecular constituents from multicomponent polymer systems by means of liquid chromatography under limiting conditions of enthalpic interactions, Eur. Polym. J., 45 (2009) 1798-1810.
[76] L. Couvreur, B. Charleux, O. Guerret, S. Magnet, Direct Synthesis of Controlled Poly(styrene-co-acrylic acid)s of Various Compositions by Nitroxide-Mediated Random Copolymerization, Macromol. Chem. Phys., 204 (2003) 2055-2063.
[77] B.J. Holland, J.L. Adcock, P.N. Nesterenko, A. Peristyy, P.G. Stevenson, N.W. Barnett, X.A. Conlan, P.S. Francis, The importance of chain length for the polyphosphate enhancement of acidic potassium permanganate chemiluminescence, Anal. Chim. Acta, 842 (2014) 35-41.

Supporting Information

for

Characterization of oligo(acrylic acid)s and their block co-oligomers

Adam T. Sutton[1,2], R. Dario Arrua[1,2], Marianne Gaborieau[3,4], Patrice Castignolles[3], Emily F. Hilder[1,2]**

[1] Future Industries Institute (FII), University of South Australia, Mawson Lakes, South Australia 5011, Australia

[2] Australian Centre for Research on Separation Science (ACROSS), School of Natural Sciences, University of Tasmania, Hobart, Tasmania 7005, Australia

[3] Western Sydney University, ACROSS, School of Science and Health, Locked Bag 1797, Penrith NSW 2751, Australia

[4] Western Sydney University, Medical Sciences Research Group, Locked Bag 1797, Penrith NSW 2751, Australia

Table of Contents

1. Size Exclusion Chromatography (SEC)

Acetic acid is necessary to ensure that the chromatograms are repeatable (i.e. to minimize adsorption of oligoacrylates; adsorption events are to be minimized in SEC). TFA has previously been added to THF mobile phase to reduces the adsorption events of poly(methacrylic acid) in a smaller quantity than that of acetic acid.[1] Therefore the use of 0.1 (w/w)% TFA in the mobile phase was compared to 5 (w/w)% acetic acid. Using 0.1 (w/w)% TFA led to repeatability comparable to that with 5 (w/w)% acetic acid. The resolution was improved and the so-called “end-of-column” void was dramatically reduced from 30-36 min to 31-32 min (Figure 1) because of the significantly lower amount of acid used. From the improvements in resolution the quantification of any unreacted RAFT agent is possible by comparing the peak area of the RAFT agent injected by itself to the peak found in the chromatogram of the sample. Using 5 (w/w)% acetic acid in the mobile phase 9 (w/w)% of unreacted RAFT was found while 13 (w/w)% was found using 0.1 (w/w)% TFA in the mobile phase. The differences in the values show that the integration error cause by the poor resolution of the RAFT agent limits the accuracy of the quantification when using acetic acid.

2. Dissolution

2.1 Dissolution monitored by free solution CE

Dissolution experimental conditions:

To monitor the dissolution of the oligoAA 2.3 mg of sample was weighed into a vial. 460 µL of water was added to the vial. 1 h later without stirring 1 mol equivalent of 1 M NaOH with respect to the acrylic acid monomer units was added to the vial. 2 hour later without stirring 10 µL of 10 % (v/v) DMSO was added as an internal standard. The sample was injected from the vial every hour for 12 hours then on later days (Figures S-1 and S-2). The CE conditions were the same as for the block co-oligomer samples except a 110 mM sodium borate buffer was used and all data processing was conducted using Chemstation A.10.01.

Results and discussion:

As the number of AA units increases the sample becomes more hydrophilic and so for a higher molar mass oligoAA the majority of the sample dissolves in water. The PABTC RAFT agent is soluble in water at very low concentrations but in low molar mass samples with average chain length of 7 AA units or lower the amount of unreacted RAFT agent is usually too high to dissolve in water. Increasing the pH of the solution improves the solubility but can lead to degradation. AA4 was dissolved in 1 mol equivalent of aqueous NaOH at a nominal concentration of 5 g L^{-1}. The dissolution in aqueous NaOH did not follow an apparent first order rate kinetics as is the case when the dissolution is solely due to the solvation of the molecule (Figure S-3).[2] That is likely due to the dissolution taking place in two steps: the initial deprotonation of the acid groups followed by the solvation of the molecule. Ensuring a dissolved sample is important for studying oligomers in aqueous systems[3, 4] and synthesizing them in alkaline aqueous solutions[5]. For the analysis of more hydrophobic block co-oligomers it is possible to incorporate an organic solvent such as methanol to the Background Electrolyte (BGE) and to dissolve the sample.

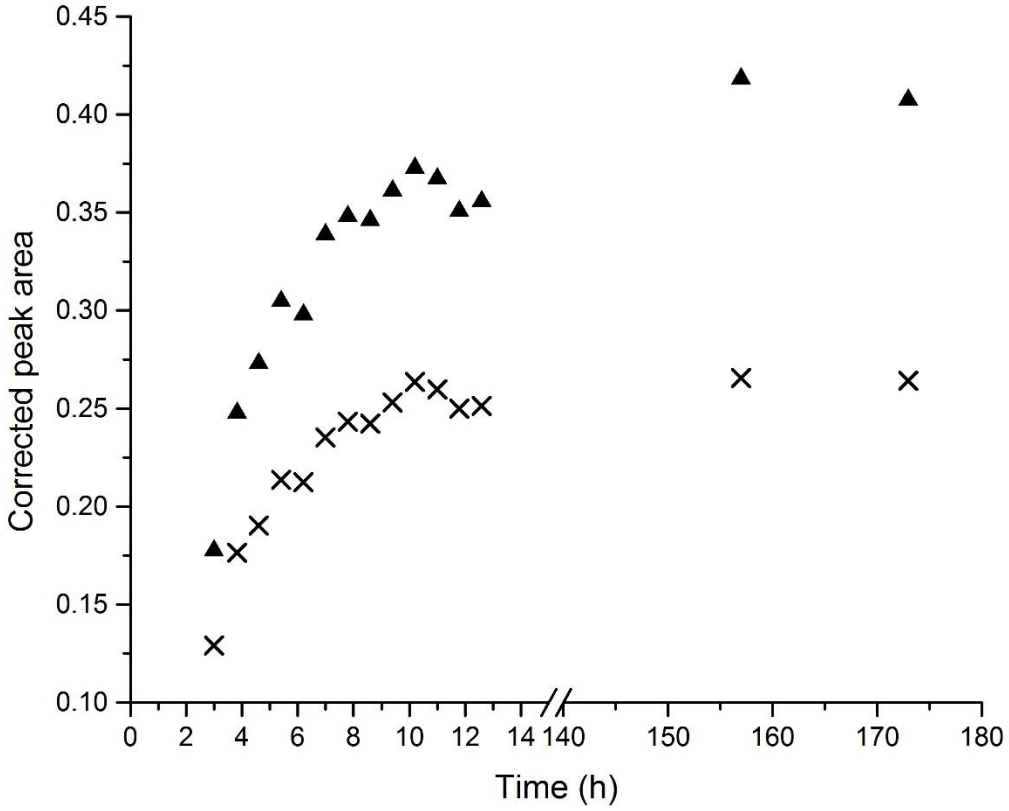

Figure S-1. Dissolution of unreacted RAFT agent (cross) and AA2R (triangle) in AA4 in water and 1 mol equivalent NaOH with respect to the AA monomer units. Concentration at complete dissolution of the AA4 sample was 5 g L^{-1} nominal concentration. Dissolution was monitored through the peak areas obtained by free solution CE.

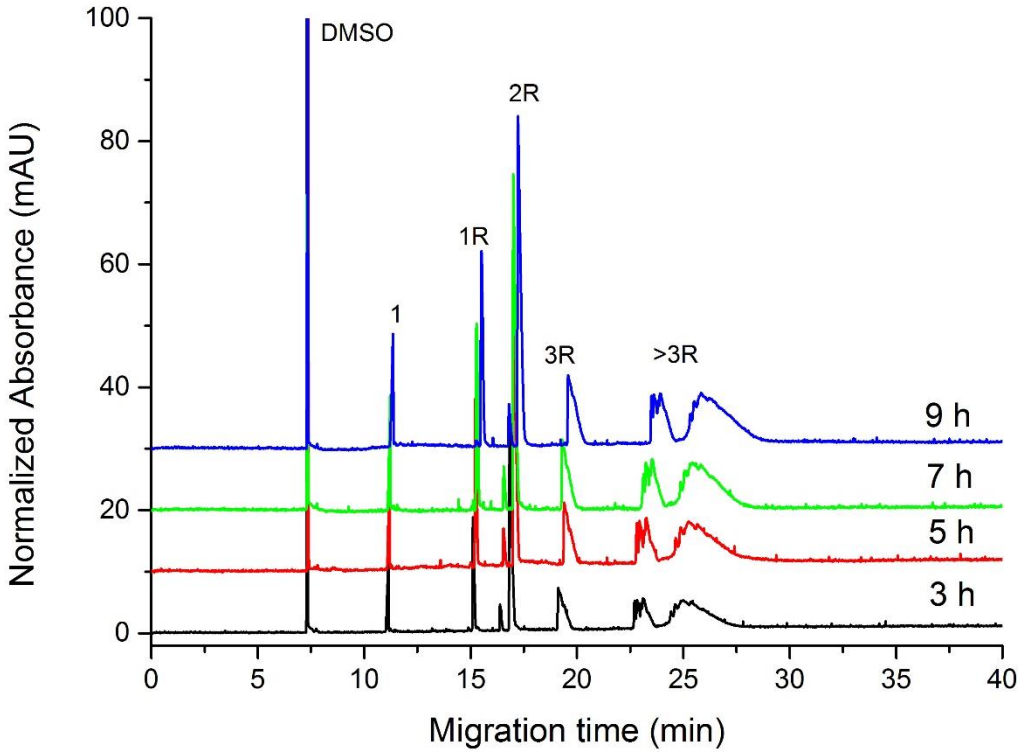

Figure S-2. Representative electropherograms of sample AA4 taken at different time intervals to monitor its dissolution. Peak areas are normalized to the peak area of DMSO internal standard. The number indicates the number of AA units, R represents a RAFT agent end group. Detection was at 200 nm.

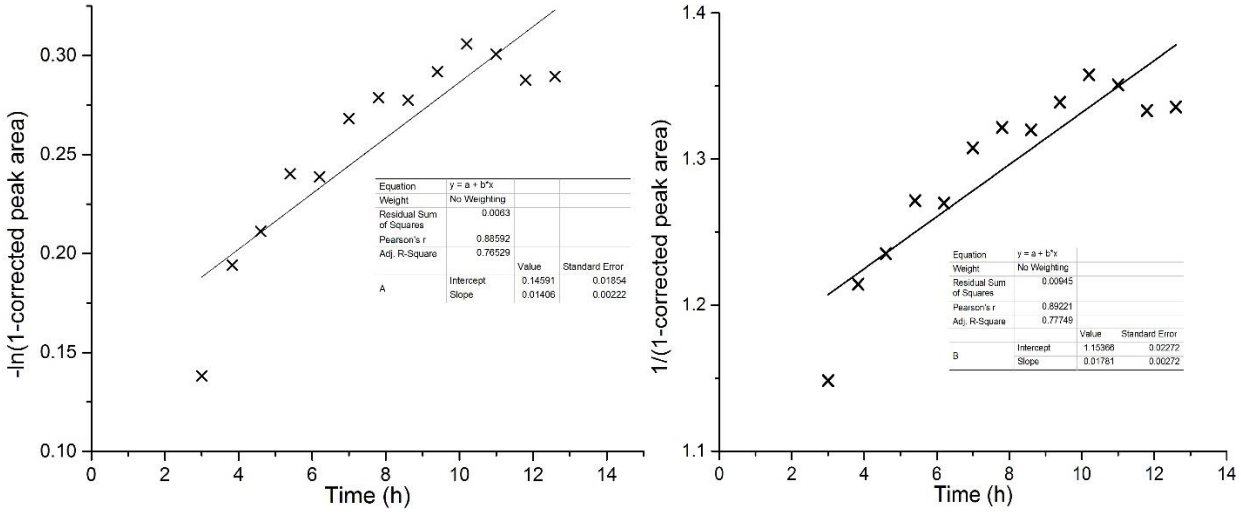

Figure S-3. Linear fitting of the dissolution of the unreacted RAFT agent as if it were following first order kinetics (left) and second order kinetics (right). Fitting information provided in the tables on the figures.

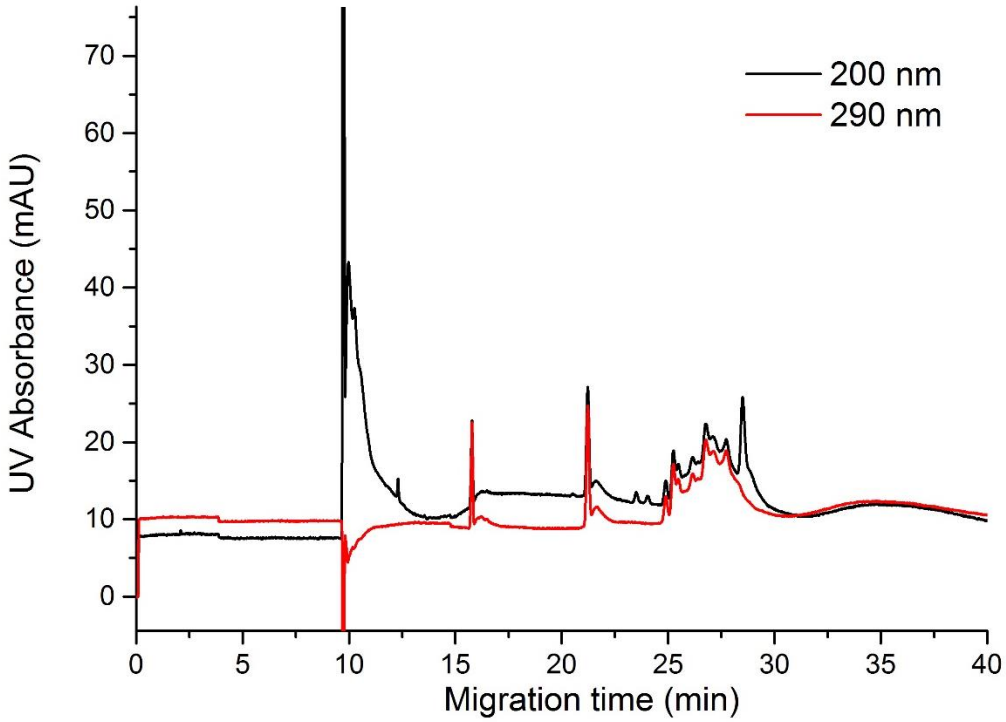

Figure S-4. Electropherogram of AA4 dissolved in dioxane to 5 g L^{-1}. Separation took place in a 59.2 cm total length capillary (50.7 cm effective length) at 25 °C with an applied voltage of 30 kV and a 400 mM lithium borate buffer. Detection was at 200 nm (black) and 290 nm (red).

2.2 Dissolution of oligo(AA-*b*-Sty) for NMR

For NMR spectroscopy of block co-oligomers samples the solvent of choice not only needs to dissolve the entire sample, the solvent signal must also not overlap with any signals of interest. Another limitation with amphiphilic samples is potential aggregation which can cause signal broadening due to aggregation which increases integration error. Such errors in NMR spectroscopy have been suggested to be of a similar magnitude to the ionization bias seen in ESI-MS.[6] Dioxane-d_8 and DMSO-d_6 caused some signal broadening, while THF-d_8 and D_2O with 1 mol equivalent of NaOD with respect to the AA monomer units resulted in more narrow signals. In addition, when a small percentage of water was present in the THF-d_8 the water signal overlapped with the backbone signals in ^{1}H NMR spectra. The signal sharpness was further improved by performing the experiments at 60 °C for D_2O (Figure S-5). The solvent signals of DMSO-d_6 and THF-d_8 overlapped with the backbone signals causing integration errors. Thus, for NMR spectroscopy block co-oligomers were analyzed in D_2O and NaOD at 60 °C. However this prevents the detection of any oligoSty and the samples cannot be dissolved at the concentrations required for ^{13}C NMR spectroscopy (>75 g L^{-1}). Therefore for ^{13}C NMR spectroscopy THF-d_8 was used as the backbone region was not required. With the choice of solvent taken into account the error on the average chain length and composition from integration errors can be significantly minimized.

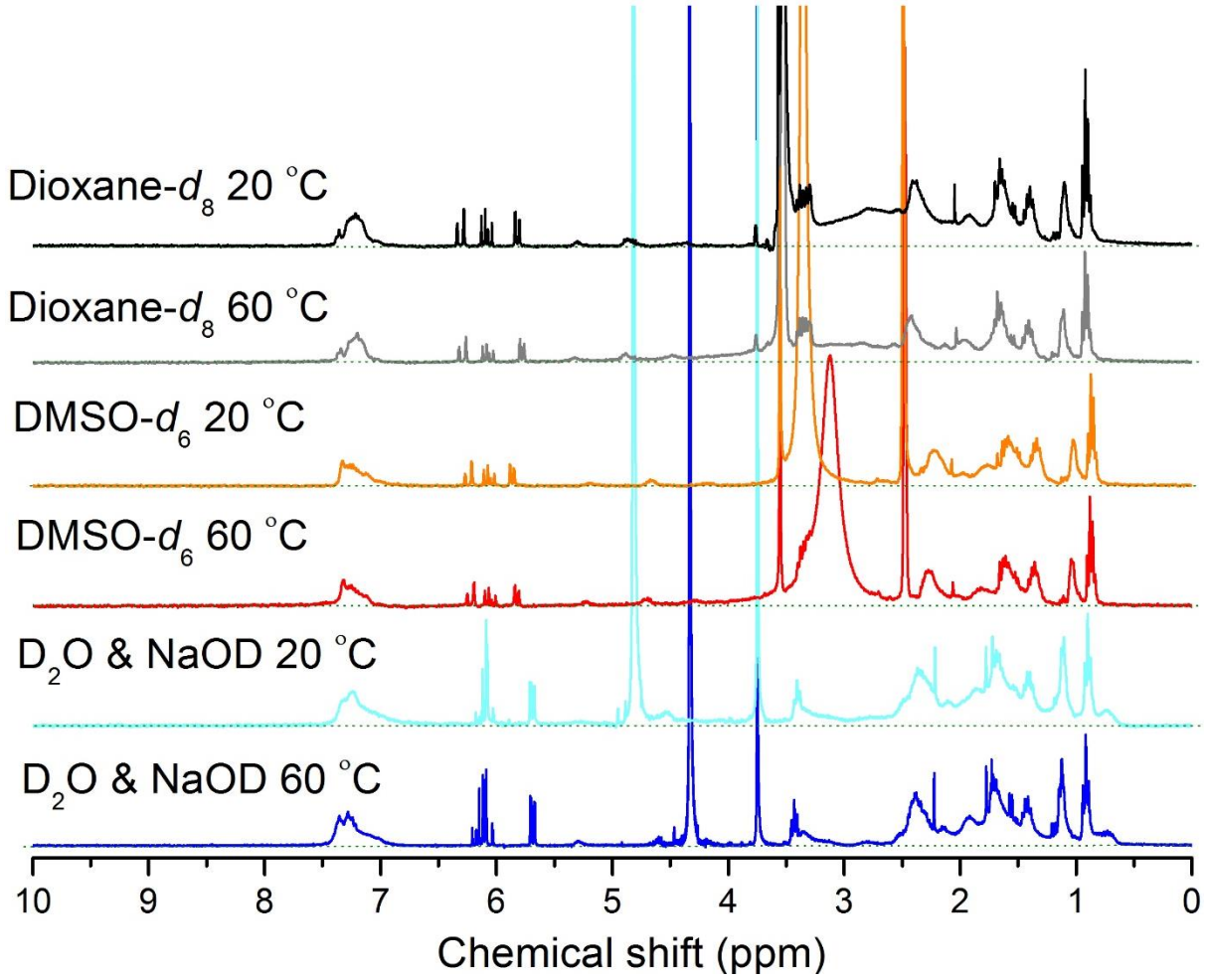

Figure S-5. Effect of solvent and temperature on ^{1}H NMR spectrum of AA4Sty1. Repetition delay was insufficient to produce quantitative spectra. Dotted lines provide visual guides to the baseline.

3. Sample Information

Table S-1. Average chain length and composition, monomer and RAFT agent conversion of oligoAA and oligo(AA-*b*-Sty) samples.

Sample code	Theoretical chain length[a]	Chain length maximum in a ESI-MS distribution[b]	Chain length NMR[c]		Conversion of RAFT agent (% mol/mol)[f]
			^{1}H[d]	^{13}C[e]	
AA3	2.87	3	ND	ND[g]	53.5 ± 5.6
AA5	4.73	5	ND	ND	ND
AA6	5.65	6	ND	ND	91.0 ± 0.4
AA10	10.30	11	11.34± 0.93	12.62 ± 0.30 [10.05 ± 1.31[h]]	ND

[a]Calculated using Equation S-8 [b]values published previously [c]calculated using Equations S-10 to S-13 [d]error calculated from the SNR using Equation S-9 [e]error based on SNR and estimated integration error [f]determined by free solution CE with n=3, absorbance at 290 nm to measure the RAFT agent, value calculated by the unreacted RAFT/total RAFT ×100 [g]ND is not determined [h]calculated using Equation S-17 which also uses H terminated end group, the error was calculated using Equation S-18

4. Capillary Electrophoresis (CE)

4.1 Equations for CE

The electrophoretic mobility (μ) was determined using Equation S-1:

$$\mu = \frac{l_\mathrm{d} l_\mathrm{t}}{V}\left(\frac{1}{t_\mathrm{m}} - \frac{1}{t_\mathrm{EOF}}\right) \qquad \text{(S-1)}$$

where l_d is the length to the detection window (effective length), l_t is the total length of the capillary, V is the applied voltage, t_m is the migration time of the analyte and t_EOF is the migration time of the electro-osmotic flow (EOF) marker.

UV absorbance was transformed using Equation S-2[7] to obtain the weight distribution of electrophoretic mobility of the sample :

$$W(\mu) = S_\mathrm{UV} \times t_\mathrm{m} \qquad \text{(S-2)}$$

Where $w(\mu)$ represents the weight distribution of electrophoretic mobiltiy of the sample and S_UV is the raw UV signal.

The correction of electrophoretic mobility of the block co-oligomer samples was conducted using Equation S-3[8]:

$$\mu_{\mathrm{corr}} = \mu \cdot \frac{\mu_{\mathrm{ref}}}{\mu_{\mathrm{mark}}} \qquad \text{(S-3)}$$

where μ_{corr} is the corrected electrophoretic mobility, μ_{ref} is the known electrophoretic mobility of the marker (which was AA4 without RAFT agent end group) and μ_{mark} is the electrophoretic mobility of the marker in the electropherogram.

Peak capacities (N_c) were estimated using Equation S-4:

$$N_{\mathrm{c}} = \frac{P_{\mathrm{w}}}{t_{\mathrm{t}}} \qquad \text{(S-4)}$$

where P_w is the peak width of a representative peak and t_t is the total time required for all the peaks to be detected. The peak width was measured at the base of the peak by taking the points where the tangents at half maximum intersect the baseline.

Weight fraction were calculated from electropherograms detected at 200 nm using Equation S-5. At 200 nm the carboxylic acid group and RAFT agent are detected. At 290 nm only the RAFT agent is detected, thus the conversion of RAFT agent was calculated using the electropherograms detected at 290 nm.

$$Weight\ fraction\ (\%) = \frac{individual\ peak\ area}{total\ peak\ areas} \times 100 \qquad \text{(S-5)}$$

The weight-average electrophoretic mobility (μ_w) was calculated using Equation S-6 as explained in reference [9].

$$\mu_{\mathrm{w}} = \frac{\sum_{\mathrm{z}} W(\mu_{\mathrm{z}})\, \mu_{\mathrm{z}}\, (\mu_{\mathrm{z+1}} - \mu_{\mathrm{z}})}{\sum_{\mathrm{z}} W(\mu_{\mathrm{z}})\, (\mu_{\mathrm{z+1}} - \mu_{\mathrm{z}})} \qquad \text{(S-6)}$$

The dispersity of the electrophoretic mobility distribution $D(1,0)$ was calculated according to Equation S-7:

$$D(1,0) = \frac{\sum_{\mathrm{z}} W(\mu_{\mathrm{z}}) \mu_{\mathrm{z}}^{-1} (\mu_{\mathrm{z+1}} - \mu_{\mathrm{z}}) \times \sum_{\mathrm{z}} W(\mu_{\mathrm{z}}) \mu_{\mathrm{z}} (\mu_{\mathrm{z+1}} - \mu_{\mathrm{z}})}{[\sum_{\mathrm{z}} W(\mu_{\mathrm{z}}) (\mu_{\mathrm{z+1}} - \mu_{\mathrm{z}})]^2} \qquad \text{(S-7)}$$

4.2 Optimization of free solution CE for oligoAA

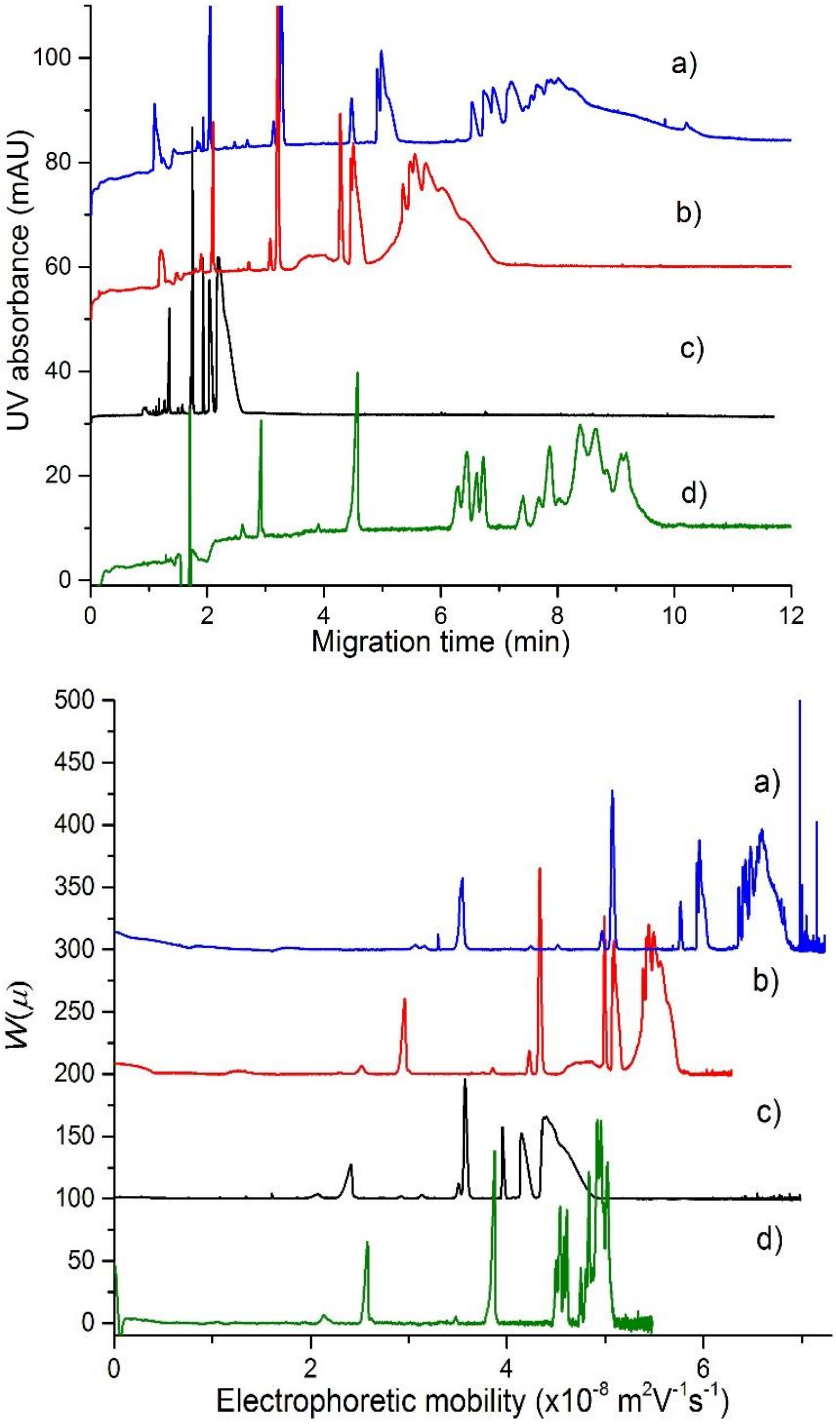

Figure S-6. Separation of AA5 using as BGEs 200 mM borate buffers with the counter ion being a) potassium (blue), b) sodium (red) and c) lithium (black) or d) 150 mM ammonium acetate (green). Electropherograms are shown as a function of migration time (top) and of electrophoretic mobility (bottom). Separations took place in a 40 cm total length capillary (31.5 cm effective length) at 25 °C and 25 kV for a) and b), 30 kV for c) and 20 kV for d). The resulting currents were 168 µA for a), 120 µA for b), 160 µA for c) and 68 µA for d). Injection concentration was 1 g L^{-1}. Detection was at 200 nm.

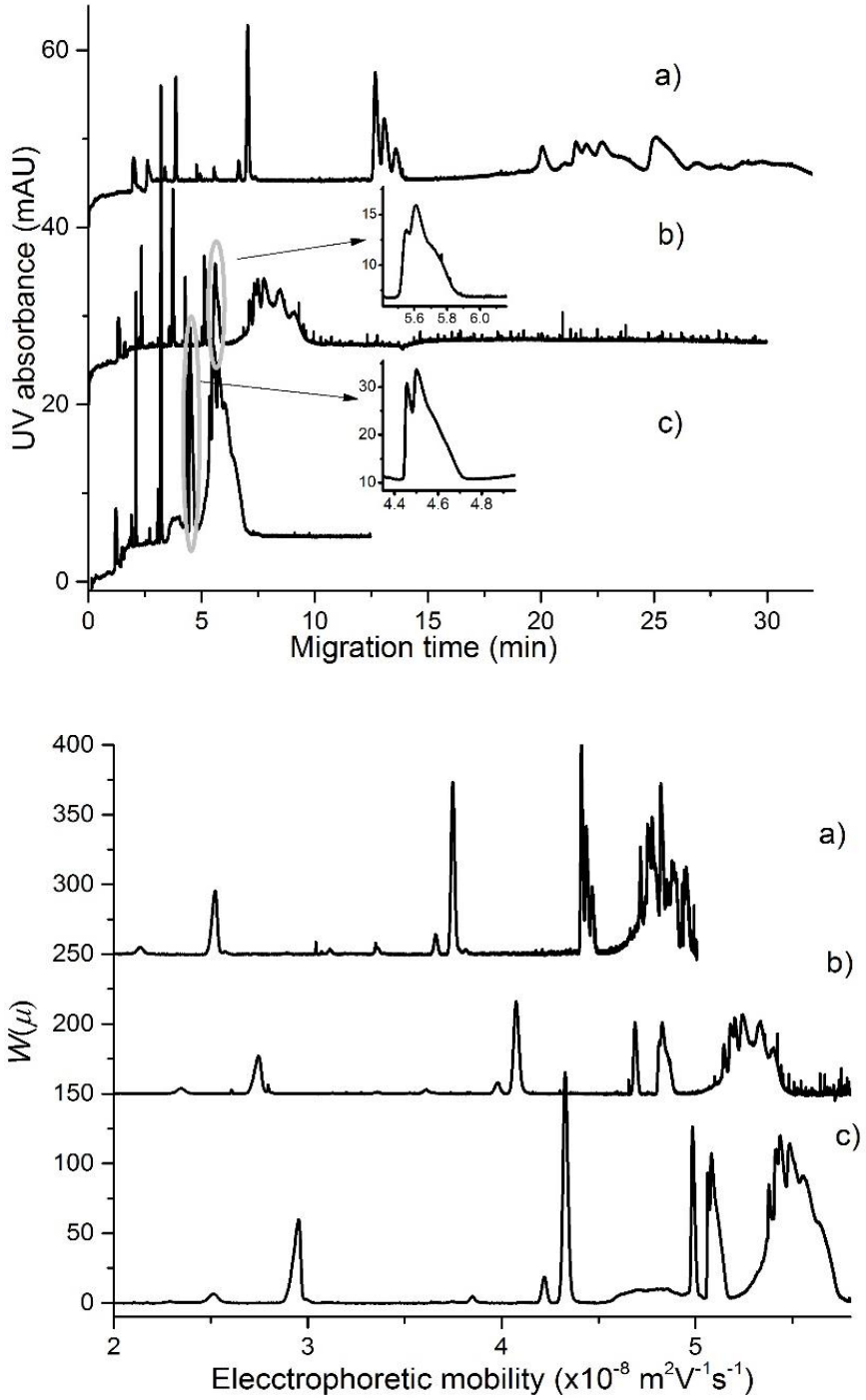

Figure S-7. Separation of AA5 with a sodium borate buffers as BGE at concentrations (a) 400 mM, (b) 300 mM and (c) 200 mM. Insert shows the peak corresponding to oligomers that are 3 monomer units long with RAFT agent end group. Electropherograms are shown as a function of migration time (top) and of electrophoretic mobility (bottom). Injection concentration was 0.5 g L^{-1}. Separations took place in a 40 cm total length capillary (31.5 cm effective length) at 25 °C and 25 kV for a) and b) or 20 kV for c). Detection was at 200 nm.

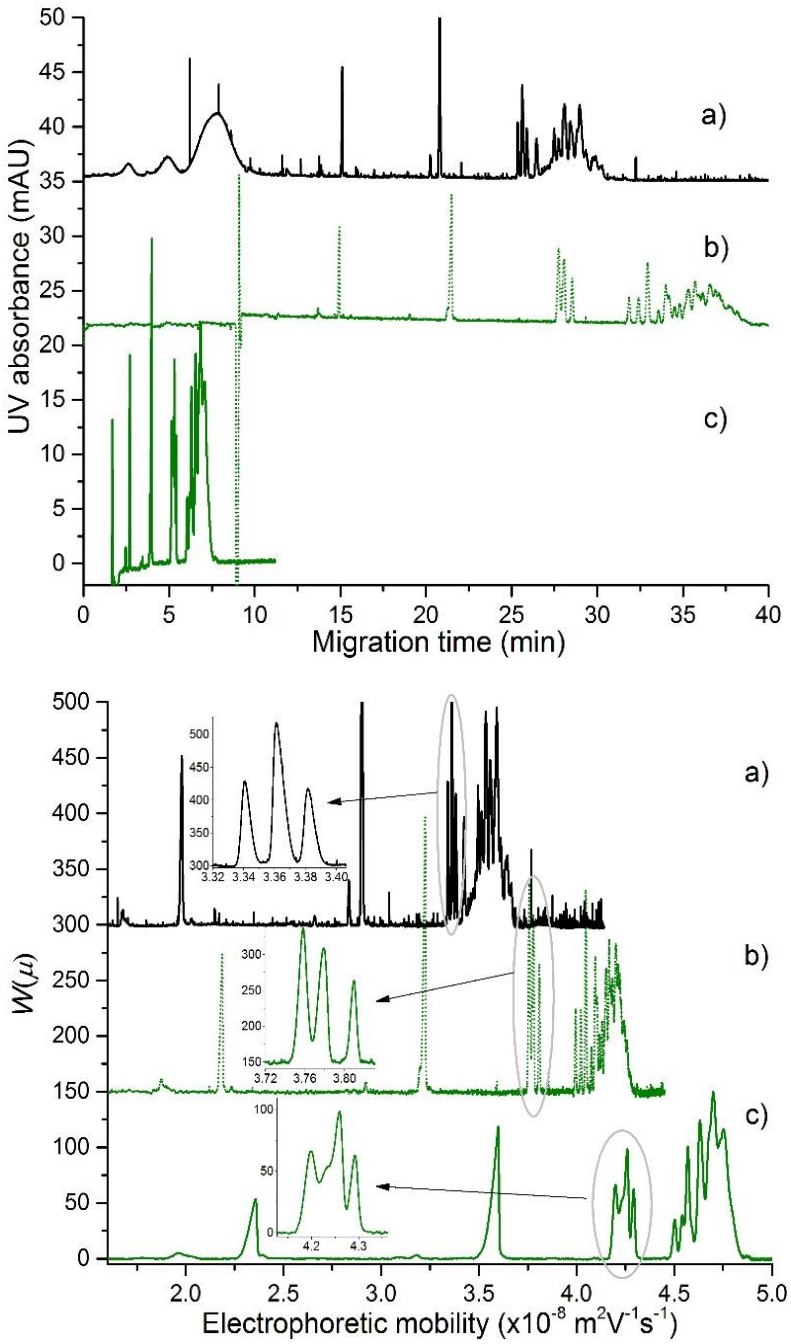

Figure S-8. Separation of AA5 in a 100 cm capillary with a 200 mM lithium borate buffer as the BGE a) (black) and 100 mM ammonium acetate b) (green dotted line), the separation with a 40 cm capillary with a 100 mM ammonium acetate is shown in c) (green full line). Insert shows the peak corresponding to oligomers that are 3 monomer units long with RAFT agent end group. Electropherograms shown as a function of migration time (top) and as a function of electrophoretic mobility(bottom). Injection concentration 1 g L^{-1}. Separations took place at 25 °C with an applied voltage of 30 kV for (a) and (b) and 20 kV for (c). Detection was at 200 nm.

4.3 Free solution CE with coated capillaries

A dynamic poly(*N*-vinyl pyrrolidone) (PVP) coating was initially applied as described previously[10], which involves flushing the capillary with 1 (w/w)% PVP during the preconditioning, as a simple way to attempt to lower the EOF. However, the coating was not stable in the examined BGEs giving no noticeable difference in the separation performance (Figure S-9).

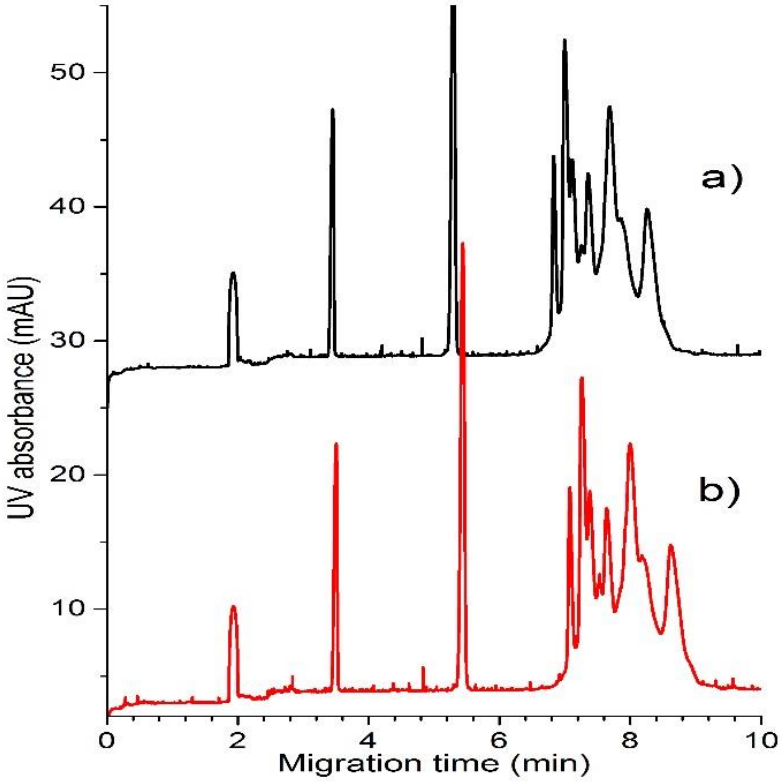

Figure S-9. Influence of the PVP dynamic coating of the bare fused silica capillary on the separation of AA5 with a 400 mM lithium borate buffer BGE; (a) no coating, (b) PVP dynamic coating. Separations took place in a 40 cm total length capillary (31.5 cm effective length) at 25 °C and 20 kV. Injection concentration was 1 g L^{-1}. Detection was at 290 nm.

A covalently grafted C18 coating was next examined according a previously described procedure.[11] The general procedure used was filling a bare fused silica capillary with a solution of 1.25 g of octadecyl trimethylsilane in 0.25 g ethanol (acidified with acetic acid to pH 5 or lower) and put in a GC oven at 110 °C. By varying the time oven the density of the coating was changed. Majority of the surface was covered by leaving the capillary in the oven overnight, a full 24 h was required to reach full coverage. The coatings were stable in the tested BGEs. A partial coating of the surface provided a slight reduction in the EOF with the EOF marker coming at 1.5 min instead of 1.0 min (Figure S-10). The separation took place in twice the amount of time but the resolution was slightly improved. Further increasing the coating coverage by extending the oven time during the coating process further lowered the EOF.

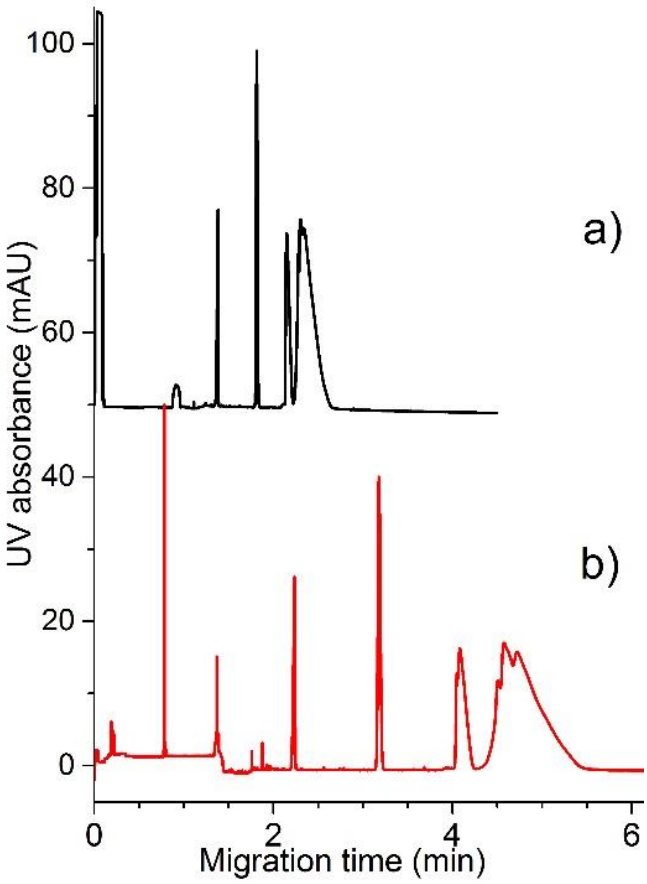

Figure S-10. Influence of a partial C18 coating of the bare fused silica capillary on the separation of AA5 with a 100 mM lithium borate buffer BGE; (a) no coating, (b) partial C18 coating. Separations took place in a 40 cm total length capillary (31.5 cm effective length) at 25 °C and 30 kV. Injection concentration was 1 g L^{-1}. Detection was at 290 nm.

Since the oligomers examined here are anionic under the conditions used, reverse polarity (the inlet and outlet polarities are switched such that the detector near the outlet is the positively charged end) is required to migrate the analytes towards the detector when no EOF is present. When using reverse polarity the oligomer migrate in reverse order so that the larger molar masses reach the detector first, this was observed when using this coating (Figures S-11 and S-12). To allow an even faster detection of the larger molar masses a coating which completely covers the surface was used. With complete coverage there is no measureable EOF. With the complete surface coated it was possible to detect the polymer chains in less than 3 min (Figure S-12).

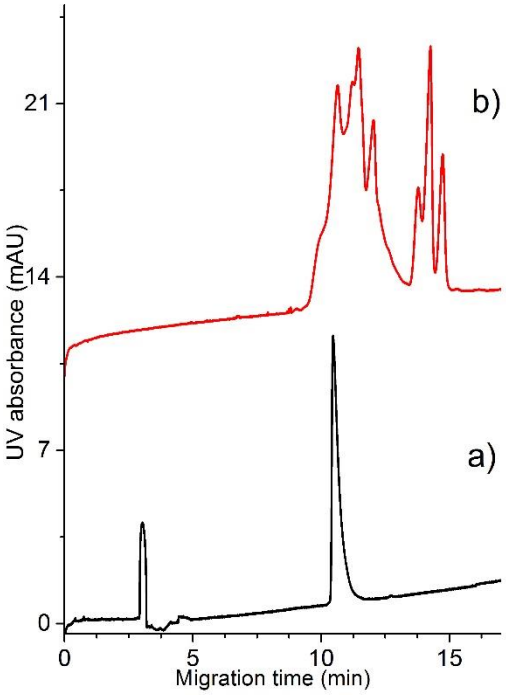

Figure S-11. Influence of a C18 coating on majority of the bare fused silica capillary surface on the separation of AA5 with a 200 mM lithium borate buffer BGE; (a) normal polarity, (b) reverse polarity. Separations took place in a 40 cm total length capillary (31.5 cm effective length) at 25 °C and 20 kV. Injection concentration was 1 g L^{-1}. Detection was at 290 nm

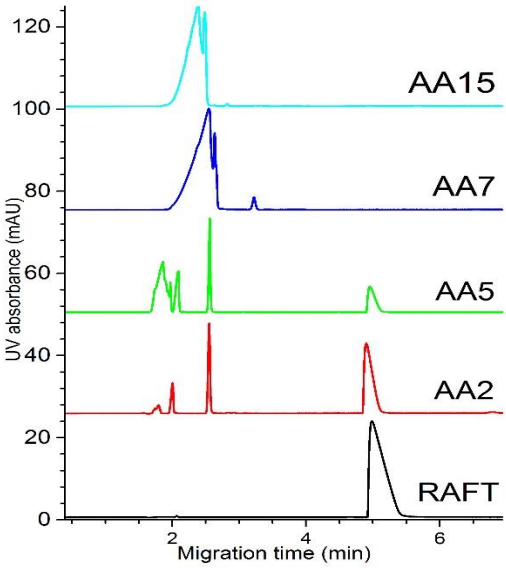

Figure S-12. Influence of full C18 coating of the bare fused silica capillary on the separation of oligoAAs with a 50 mM lithium borate buffer BGE. The oligoAA samples are of increasing average molar mass from bottom to top with the number indicating the most intense peak in an ESI-MS spectrum determined previously *[12]*. Separations took place in a 40 cm total length capillary (31.5 cm effective length) at 25 °C and -20 kV. Injection concentration was 1 g L^{-1}. Detection was at 290 nm.

Applying a C18 coating requires a day of preparation and such equipment may not be readily available to materials laboratories therefore a capillary made from fluorinated ethylenepropylene copolymer was looked at as an alternate type of capillary that has a reduced EOF and can be simply purchased.[13] Although this capillary was able to successfully reduce the EOF it suffered from poorer heat dissipation and an inability to maintain high currents (>100 µA) preventing the use of high concentration BGEs and high electric field strengths (Figure S-13). Therefore, the polymer chains can be detected in 5 min while the RAFT agent could not be detected in less than 30 min.

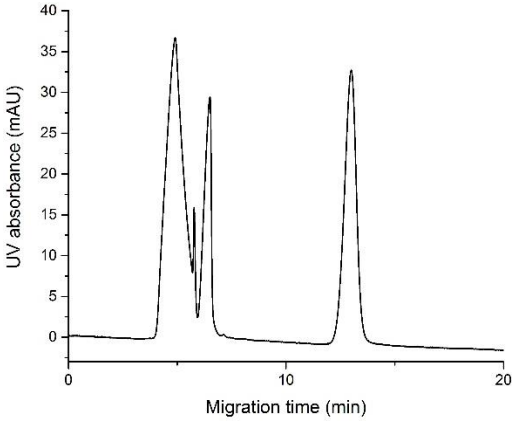

Figure S-13. Separation of AA5 with a 50 mM lithium borate buffer BGE in a 40 cm total length fluorinated ethylenepropylene copolymer capillary (effective length 31.5 cm). Separation was at 25 °C and -20 kV. Injection concentration was 1 g L^{-1}. Detection was at 290 nm.

4.4 Free solution CE with organic modifiers

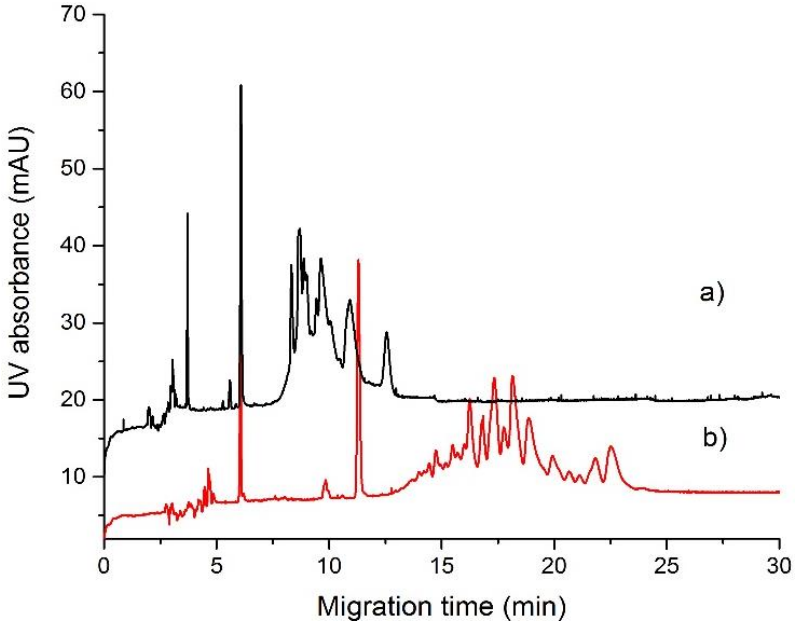

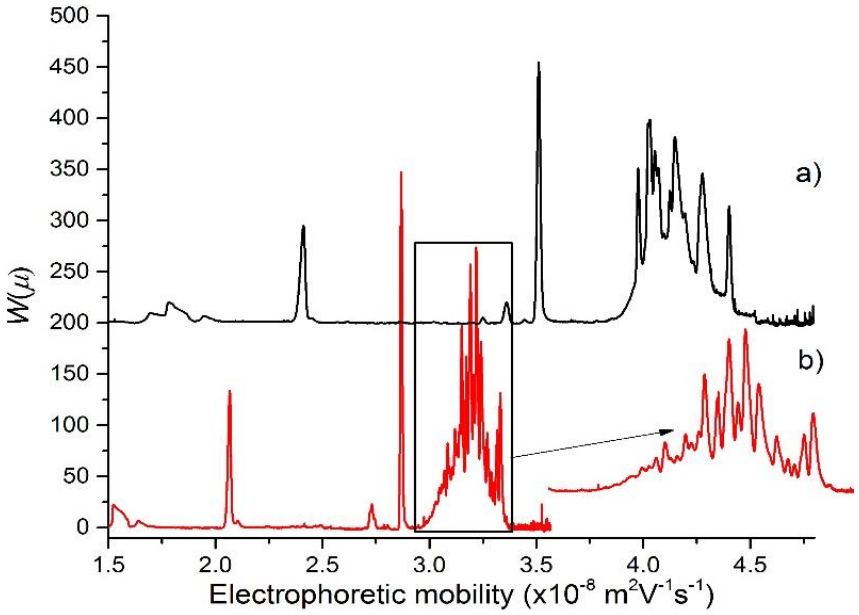

Figure S-14. Separation of AA5 with a 500 mM lithium borate buffer as the BGE at concentrations (a) without and (b) with methanol in a volume ratio of 90:10. Insert shows the peaks corresponding to higher molar mass oligomers. Electropherogram are shown as a function of migration time (left) and of electrophoretic mobility (right). Injection concentration was 1 g L^{-1}. Separations took place in a 40 cm total length capillary (31.5 cm effective length) at 25 °C and 20 kV. Detection was at 200 nm.

5. Nuclear Magnetic Resonance (NMR) Spectroscopy

5.1 Signal assignment

The signals corresponding to the RAFT agent end group are easily identified with ^{1}H NMR spectroscopy as they produce clear splitting patterns. However the backbone signals do not give well defined splitting patterns as their distance from the end group and stereochemistry change their chemical shift. The chemical structures detected by NMR spectroscopy are shown in Figure 3 with the numbers being used for peak labelling in the NMR spectra. The overlapping quartet corresponds to the equivalent signal in unreacted RAFT agent present in the sample. The quartet is correlated to a doublet (1.53 ppm) on top of the backbone signals in the COSY (Figure S-27) therefore the doublet corresponds to the methyl group of the AA unit in the unreacted RAFT agent (GN1). This doublet is also observed in the block co-oligomer samples and AA3 and AA5. The backbone signals of the larger molar mass oligoAA is too broad to detect the doublet, furthermore from free solution CE it is observed that little or no unreacted RAFT agent is present in these samples. The signal between 4.70 and 4.95 ppm is correlated to the signals between 1.8 and 2.2 ppm meaning they are related to the CH_2 signal of the AA unit next to the RAFT end group (GN13). The range of chemical shifts of the signals is due to the stereochemistry, the more downfield signals correspond to the meso isomers while the upfield signals correspond to the racemic isomers.[14]

The methyl group from the start group of the oligoAA produces a signal at 1.0 to 1.2 ppm (GN1). The downfield small signals of the methyl group are caused by short oligoAA chains with less than 3 units long as they are shown to correlate to the shoulder at 2.5 ppm which is then correlated to the AA unit next to RAFT agent end group (GN5) in the COSY (Figure S-27). The downfield shoulder of the CH backbone signal is from the second monomer unit from the RAFT end group and the CH signal of the start group (GN2) as shown by the COSY. The singlet at 2.05 ppm is not reproduced when other deuterated solvents were used and so it is likely an impurity whose peak area can be easily subtracted from that of the backbone region as it is a sharp signal only overlapping with GN13.

The signals found in oligoAA are present in the block co-oligomer samples but they are less resolved due to the sample being more complex (Figure 4b). GN14 is still present in the block co-oligomer sample indicating that some chains have not undergone chain extension as they still have an AA unit next to the RAFT agent end group. There is no significant difference in the AA content so the detected GN14 is not due to the addition of more AA units. A quartet like signal is superimposed to this signal which corresponds to the unreacted RAFT agent. Two signals are produced which both correspond to the CH of a Sty unit next to the RAFT agent end group, which has been previously observed in styrene units next to electronegative end groups[15, 16], the reason is likely due to the different stereochemistry of the unit next to the end group.

Using ^{1}H-^{13}C HMQC (Figure S-28) the signals of the backbone and RAFT agent end group could be identified in the ^{13}C spectrum and confirmed using a DEPT-135 spectrum. A number of shoulders are present between 28 and 35 ppm in Figure 5a. Two of these shoulders at 31.5 and 33.2 ppm are shown to be methylene signals in the DEPT-135 and were previously identified to be from H terminated end groups.[14, 17] The HMQC shows that the corresponding signals for the H terminated end groups in the ^{1}H spectra are overlapping with the backbone signals. The other shoulders present have a similar chemical shift to those reported for the initiator (V-501) although a different solvent was used it was not expected to influence the chemical shift by a significant amount.[18] The other signals corresponding to the other ^{13}C nuclei of the initiator were also identified and their corresponding signals in the ^{1}H spectra were shown by the HMQC to have chemical shifts similar to what was previously reported as well.[18] Typically the sensitivity of NMR spectroscopy is insufficient for the detection of initiator signals[14], however, oligomers have a higher ratio of transfer agent to initiator, in this this case 10:1, compared to the synthesis of higher molar mass polymers. Furthermore the low molar mass of oligomers means that when dissolving an equivalent mass of oligoAA to PAA the number of macromolecules is higher leading to the detection of initiator which may affect the accuracy of the chain length measurement if the initiator signals are not accounted for. The initiator signals in the ^{1}H spectra cannot be clearly observed due to overlap in the back bone region, but their peak area could lead to errors in determining the chain length. The initiator signals are only detected in oligoAA samples with an average chain length less than 5 monomer units long and the block co-oligomer samples and thus the initiator signals are negligible for most oligoAA samples. GN24 is from the quarternary carbon adjacent to the azo group in initiator (see Figure 3). The presence of GN24 indicates that the initiator detected is from non-decomposed initiator. The peak areas of GN24 and GN26 are experimentally the same indicating an undetectable amount of initiator had decomposed. The signals in the carbonyl region between 170 and 180 ppm were assigned

according chemical shifts given previously for PAA synthesized by RAFT polymerization.[14] As mentioned above, larger molar mass oligoAA samples are soluble in water. AA9 and AA21 were analyzed by free solution CE previously and it was observed that there was a small amount of unreacted RAFT which is the most difficult component of the sample to completely dissolve in aqueous solvents. Therefore D_2O was used to analyze these samples instead of dioxane-d_8. The different NMR solvent gives slight changes in chemical shift but the same profile is observed. The signals corresponding to the H terminated end group were more resolved when D_2O was used as the solvent and gave similar chemical shifts as what has been reported previously.[19]

All the signals of the AA4 are found in the ^{13}C NMR spectra of the block co-oligomer sample (Figure 5b), although the initiator signals and those from the unreacted RAFT agent are present with a lower intensity. The broadening of the backbone signals prevents the quantification of H terminated signals and initiator. The aromatic signals from the Sty units are present between 120 and 150 ppm.

No acrylic acid dimers could be detected unlike for other polymerizations involving acrylic acid.[14, 20] No *β*-scission or recombination products were detected in the oligoAA or oligo(AA-*b*-Sty) within the sensitivity of the NMR measurements based on the signals reported previously and Chemdraw chemical shift predictions.[15, 21, 22] Furthermore H terminated end groups from Sty units were not detected.[21, 22]

5.2 T_1 estimations

T_1 values were overestimated using the inversion recovery pulse sequence shown in Figure S-15. Phasing the spectra the same way as a conventional ^{13}C NMR spectrum recorded in the same conditions, each signal is negative for short delay values, positive for long delay values, with a zero crossing occurring at a τ value of $T_1 \times \ln 2$.[23] When the delay τ is sufficient to produce a positive signal, an overestimated T_1 value can thus be determined as $\tau \times 1.44$

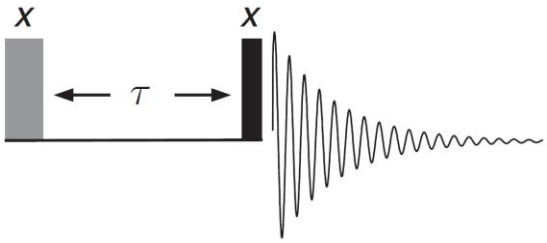

Figure S-15. One-dimensional T_1 inversion recovery pulse sequence used to estimate T_1 for ^1H NMR. The corresponding pulse sequence for ^{13}C also contains a decoupling of the hydrogen nuclei during acquisition as described in *[23]*.

5.3 Equations used to calculate average chain length and composition

The theoretical chain length was estimated using Equation S-8:[24]

$$Theoretical\ chain\ length = \frac{M_0 - M_t}{RAFT + df(I_0(1 - e^{k_d t}))} \qquad \text{(S-8)}$$

where RAFT refers to the initial RAFT agent concentration, M_0 is the initial monomer concentration, M_t is the monomer concentration remaining at time t, I_0 is the initial initiator concentration, d is the average number of chains formed from each radical–radical termination event (since disproportionation products were not detected in the NMR spectra the value was taken as 1), f is the initiator efficiency which was 0.68 from reference [25] (value was determined in acetone at 70 °C thus it is assumed have little difference to the conditions used here), k_d is the initiator decomposition constant which was extrapolated to be 9.28×10^{-6} s^{-1} from reference [26].

The Relative Standard Deviation (*RSD*) of the peak area of NMR signals was calculated from the Signal-to-Noise Ratio (*SNR*) of the chain end signal using Equation S-9 which has been determined empirically previously.[27] The SNR of the chain end signal is determined using the 'sino real' command in the Bruker Topspin software.

$$RSD\ (\%) = \frac{238}{SNR^{1.28}} \qquad \text{(S-9)}$$

The average chain length (DP_n) was calculated using the following equations.

$$DP_n = \frac{all\ monomer\ units}{all\ end\ groups} \qquad \text{(S-10)}$$

For ^{1}H spectra of oligoAA dissolved in dioxane-d_8 GN14 (GN refers to Group Number as labelled in Figure 3 and Figure 5) was used to represent the end groups as

$$DP_n = \frac{I(1.3-2.7\ ppm) - 7I(GN14)}{3I(GN14)} \qquad \text{(S-11)}$$

For ^{1}H spectra of oligoAA in dioxane-d_8 for taking into account the overlapping impurity signal and initiator signals:

$$DP_n = \frac{I(1.3-2.7\ ppm) - 7I(GN14) - I(impurity) - 1.4I(GN14)}{3I(GN14)} \qquad \text{(S-12)}$$

No initiator signals could be baseline resolved in ^{1}H spectra but the ^{13}C spectra show that the ratio of initiator to RAFT agent is 1:10 which is in agreement with the theoretical ratio. Therefore the overlapping initiator signals in the ^{1}H spectra are equal to 1.4 times the peak area of signal 14.

For ^{1}H spectra of oligoAA and oligo(AA-*b*-Sty) in D_2O with and without NaOD the HDO signal overlaps with GN14 while GN17 is clearly resolved (Figure S-5). In the oligo(AA-*b*-Sty) samples GN17 is broader with a sharper signal superimposed on top but the COSY of the sample indicates that it corresponds to a single signal (Figure S-29). Therefore Equation S-13 was used to calculate DP_n for these spectra:

$$DP_{\mathrm{n}} = \frac{I(0.5-3.0\ ppm)-3.5I(GN17)-0.7I(GN17)}{1.5I(GN17)} \qquad \text{(S-13)}$$

For ^{1}H spectra oligo(AA-*b*-Sty) where THF-d_8 is the solvent Equation S-13 was used as well except the overlapping solvent signal was subtracted using a blank spectrum of the solvent.

For ^{13}C NMR spectra a number of end group signals are resolved but the most accurate and precise DP_n comes from using the signal which is baseline resolved and has the highest SNR. Therefore S20 was used for all solvents as it was confirmed by HMQC to not be overlapping with any other signals, thus Equation S-14 was used to calculate DP_n:

$$DP_{\mathrm{n}} = \frac{I(25-55\ ppm)-2I(GN20)}{2I(GN20)} \qquad \text{(S-14)}$$

For short chain length oligomers such as AA4 the initiator signals are detected and overlap with the region stated in Equation S-14, therefore the initiator signals need to be accounted for using Equation S-15:

$$DP_{\mathrm{n}} = \frac{I(25-55\ ppm)-2I(GN20)-2I(GN26)}{2I(GN20)} \qquad \text{(S-15)}$$

Since with ^{13}C the H terminated end group can be identified this signal was added to the DP_n calculation to improve the accuracy. For spectra in dioxane-d_8 GN11 corresponding to the H terminated end group is overlapping with GN18 and GN23. Therefore Equation S-16 was used:

$$DP_{\mathrm{n}} = = \frac{I(25-55\ ppm)-2I(GN20)-2I(GN26)}{2I(GN20)+[I(25-32\ ppm)-I(20-25\ ppm)]} \qquad \text{(S-16)}$$

Only longer chain oligomers were dissolved in D_2O and so the initiator signals are not detectable, while GN11 is more resolved. However, branching is also detected in these oligomers which generates an H terminated end group thus Equation S-17 was used for these spectra:

$$DP_{\mathrm{n}} = \frac{I(25-55\ ppm)-2I(GN20)}{I(GN20)+[I(GN11)-I(GN8)]} \qquad \text{(S-17)}$$

The error can be determined for the DP_n calculation in Equation S-17 using Equation S-9 on the small signals in the denominator (first 3 terms) plus incorporating the integration error as explained in the main article (last term in equation). This is shown in Equation S-18:

$$SD(DP_n) = I(GN20)\frac{238}{SNR(GN20)^{1.28}} + I(GN8)\frac{238}{SNR(GN8)^{1.28}} + I(GN11)\frac{238}{SNR(GN11)^{1.28}} + 0.07I(GN11) \quad \text{(S-18)}$$

Where *SD* is the standard deviation.

The Sty fraction was calculated as follows:

$$Sty\ fraction = \frac{Sty\ units}{Sty\ units + AA\ units} \quad \text{(S-19)}$$

For ^{1}H spectra:

$$Sty\ fraction = \frac{0.2I(GN30)}{I(0.5-3.0\ ppm) - 3.5I(GN17)} \quad \text{(S-20)}$$

For ^{13}C spectra:

$$Sty\ fraction = \frac{0.2I(GN29)}{I(170-180\ ppm) + 0.2I(GN29)} \quad \text{(S-21)}$$

6. NMR Spectra

6.1 Spectra for T_1 estimations

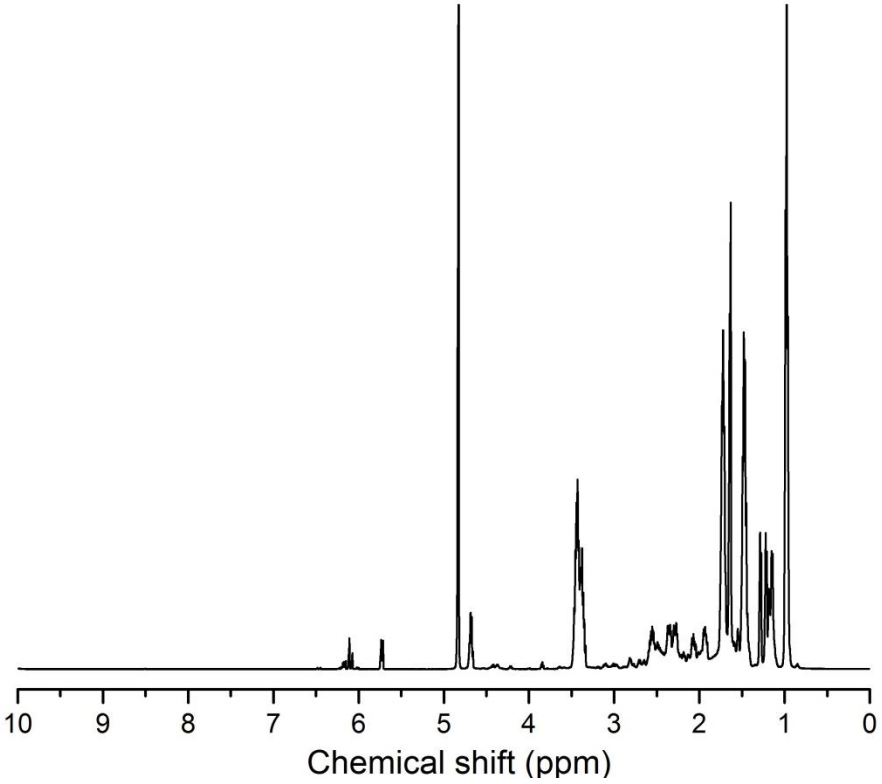

Figure S-16. ^{i}H NMR spectrum of AA3 dissolved in D_2O obtained by an inversion recovery pulse sequence showing an overestimation of the T_1 value for all signals to be 4 s.

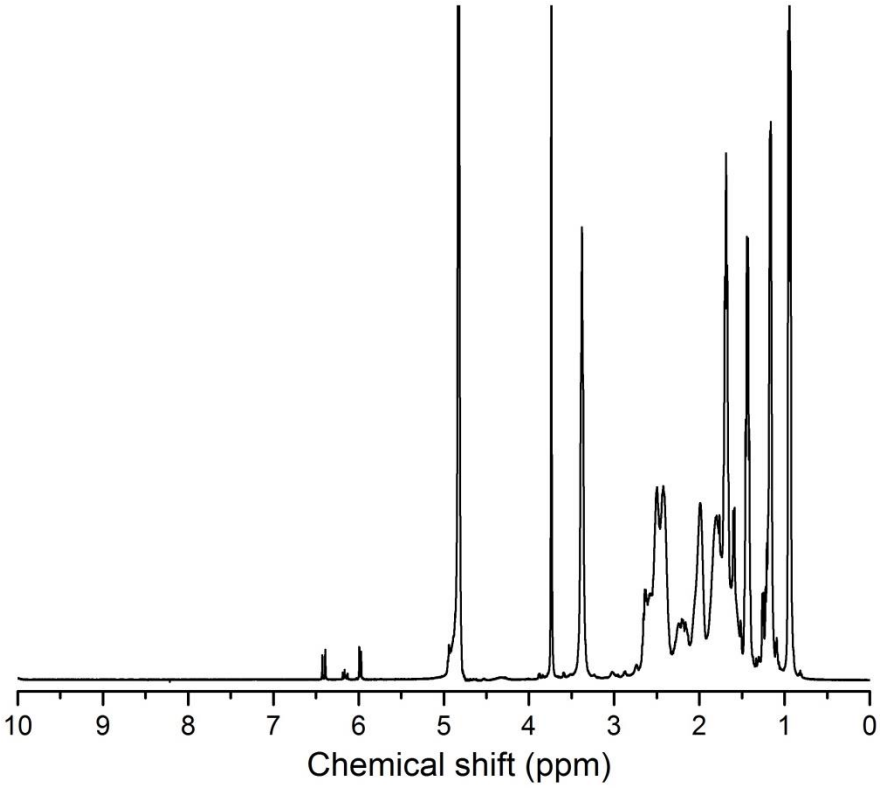

Figure S-17. ^{i}H NMR spectrum of AA5 dissolved in D_2O obtained by an inversion recovery pulse sequence showing an overestimation of the T_1 value for all signals to be 4 s.

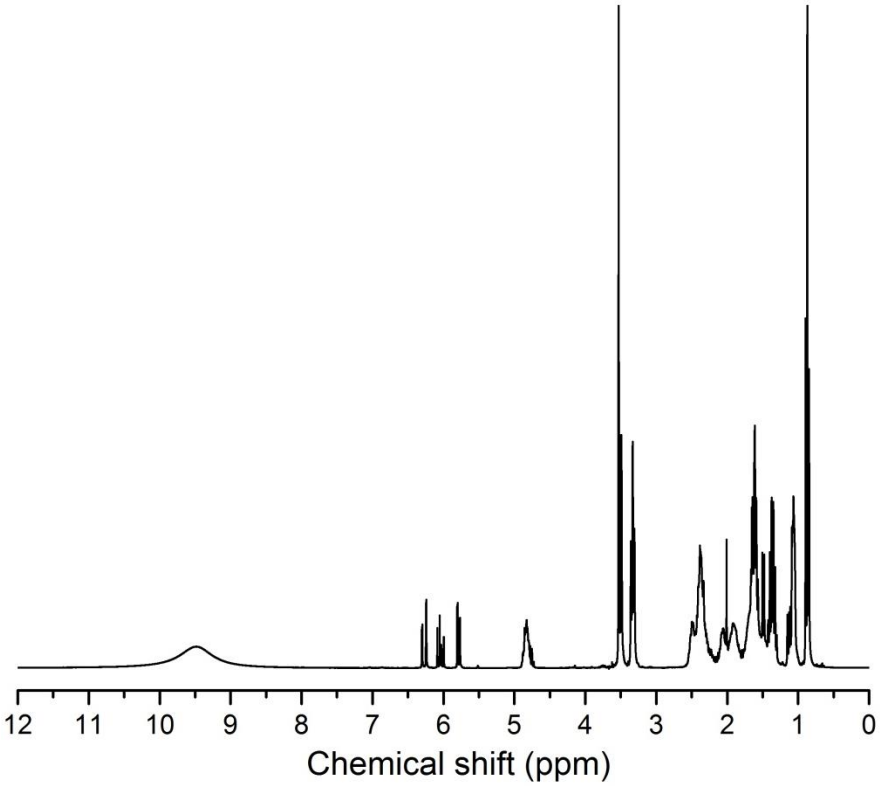

Figure S-18. ^{i}H NMR spectrum of AA4 dissolved in dioxane-d_8 obtained by an inversion recovery pulse sequence showing an overestimation of the T_1 value for all signals to be 5 s.

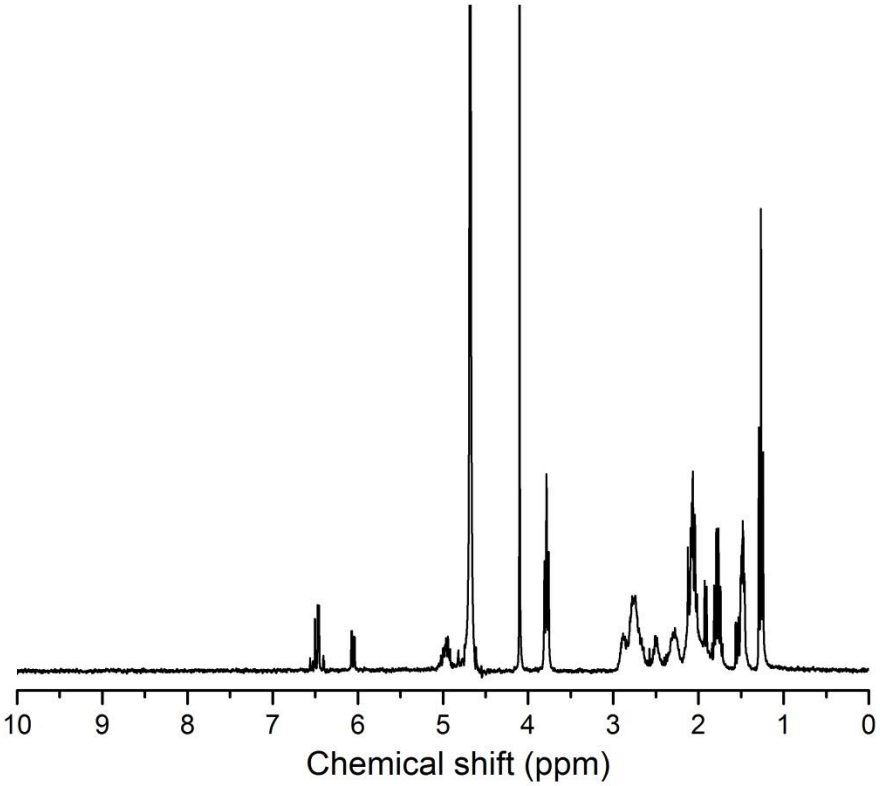

Figure S-19. ^{i}H NMR spectrum of AA4 dissolved in D_2O with 1 mol equivalent of NaOD with respect to the AA units obtained by an inversion recovery pulse sequence showing an overestimation of the T_1 value for all signals to be 5 s.

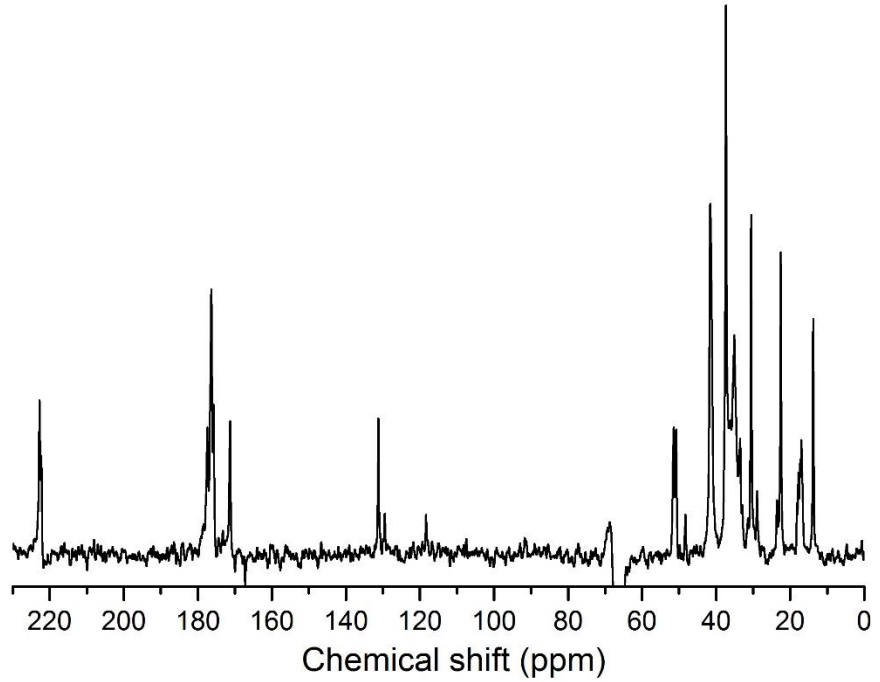

Figure S-20. ^{13}C NMR spectrum of AA4 dissolved in dioxane-d_8 with respect to the AA units obtained by an inversion recovery pulse sequence showing an overestimation of the T_1 value for all signals to be 5 s (except for the solvent signal at 66.5 ppm and the signal of the carbonyl of the residual acrylic acid monomer at 167.1 ppm).

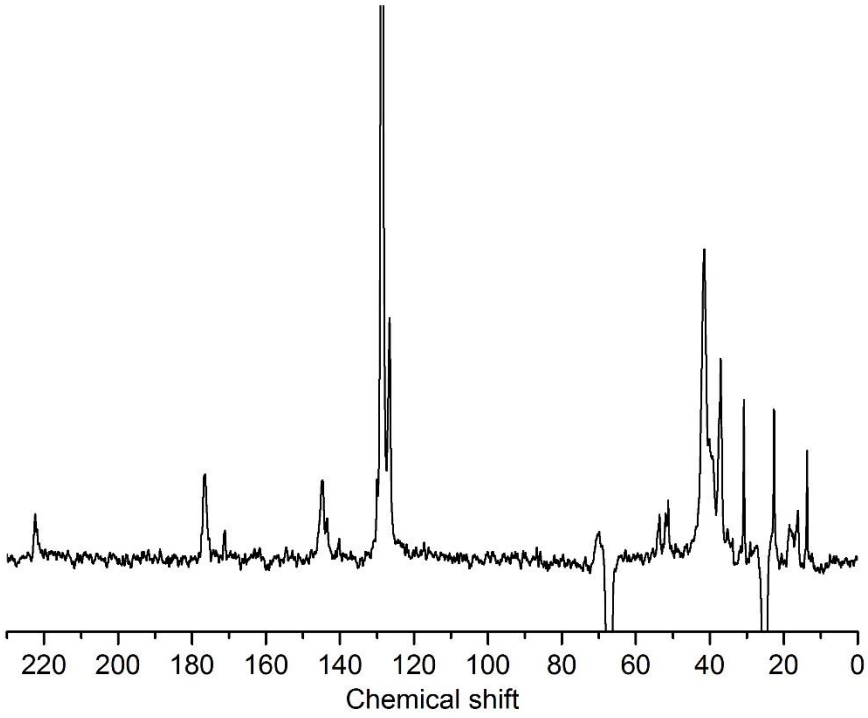

Figure S-21. ^{13}C NMR spectrum of AA4Sty3 dissolved in THF-d_8 with respect to the AA units obtained by an inversion recovery pulse sequence showing an overestimation of the T_1 value for all signals to be 5 s (except for the solvent signals at 25.5 and 67.2 ppm).

6.2 Spectra for branching identification in oligoAA

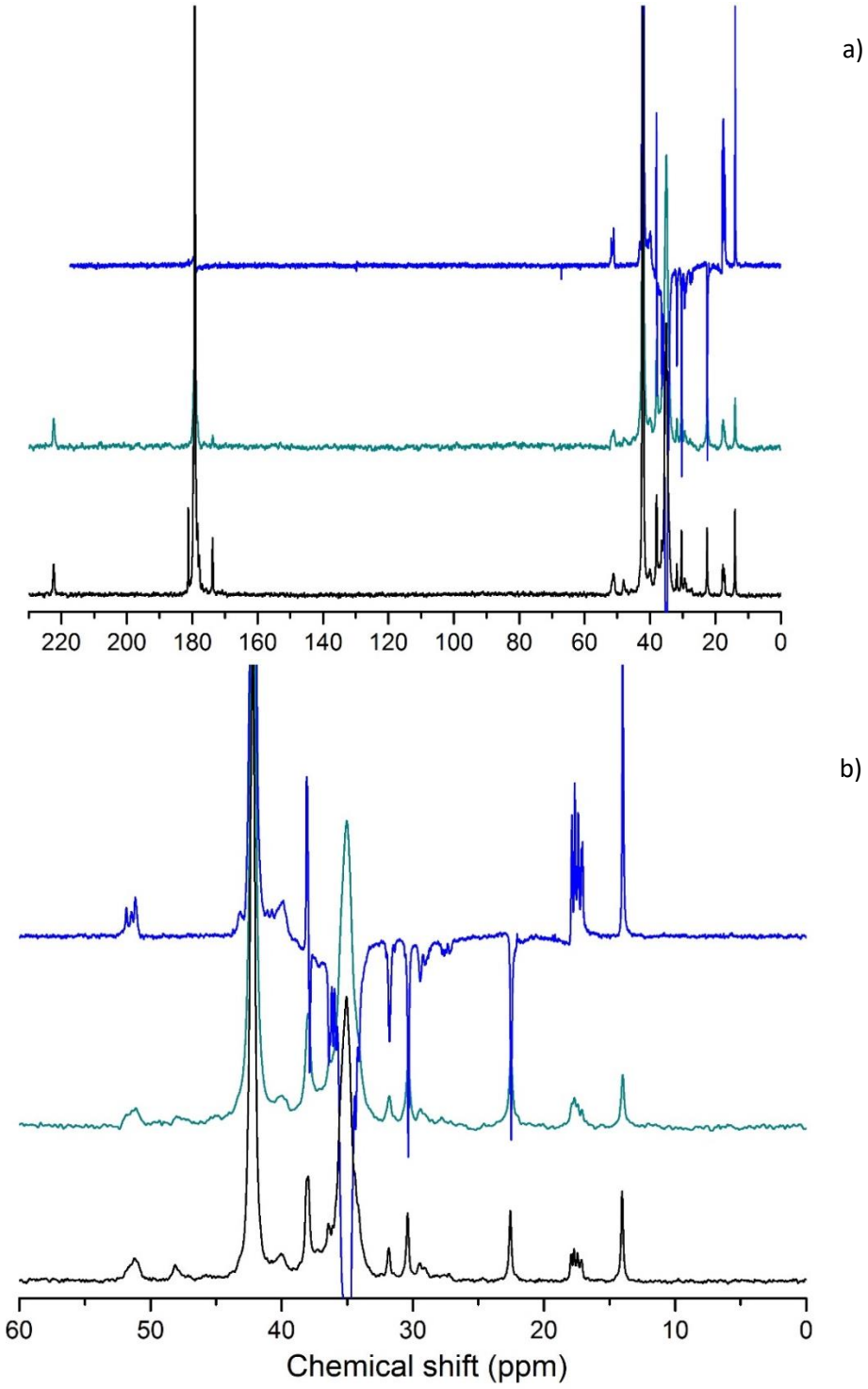

Figure S-22. ^{13}C NMR of AA21 dissolved in D_2O. a) shows full spectra and b) the spectra between 0 and 60 ppm. The bottom (black) spectra are quantitative ^{13}C spectra obtained by an inverse-gated decoupling sequence, the middle (green) ones are ^{13}C spectra obtained by inverse recovery pulse sequence showing overestimated T_1 values for all signals to be 3 s, the top (blue) ones are ^{13}C DEPT-135 spectra.

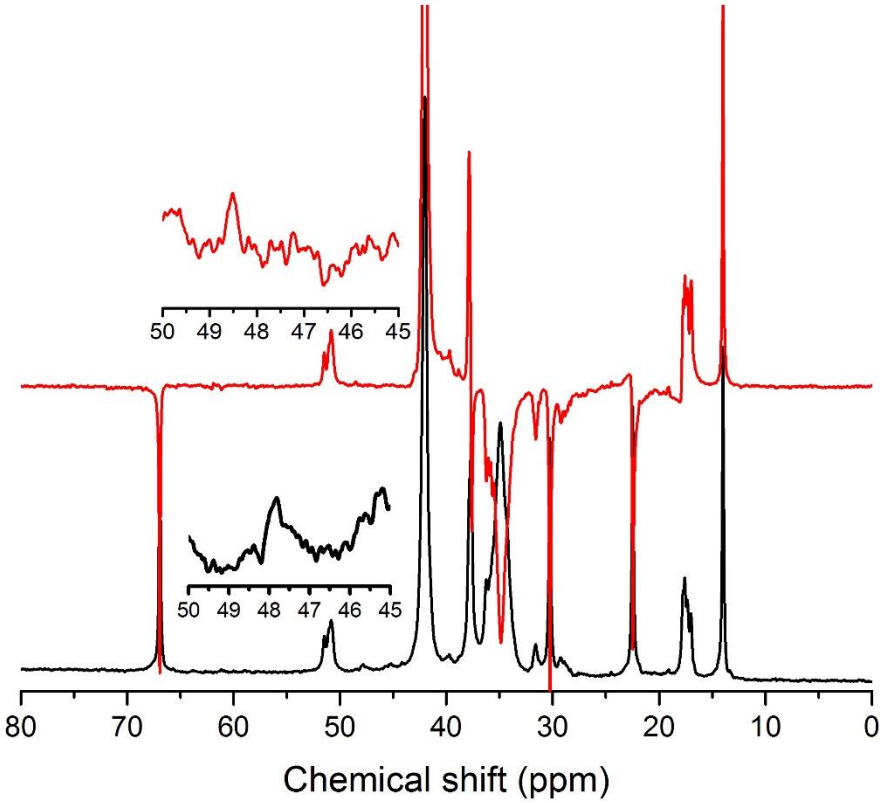

Figure S-23. ^{13}C NMR of AA9 dissolved in D_2O. The bottom (black) spectrum is a quantitative ^{13}C spectrum obtained by an inverse-gated decoupling sequence, the top (red) one is a ^{13}C DEPT-135 spectrum. Insert shows region where the quaternary carbon from the branching point appears.

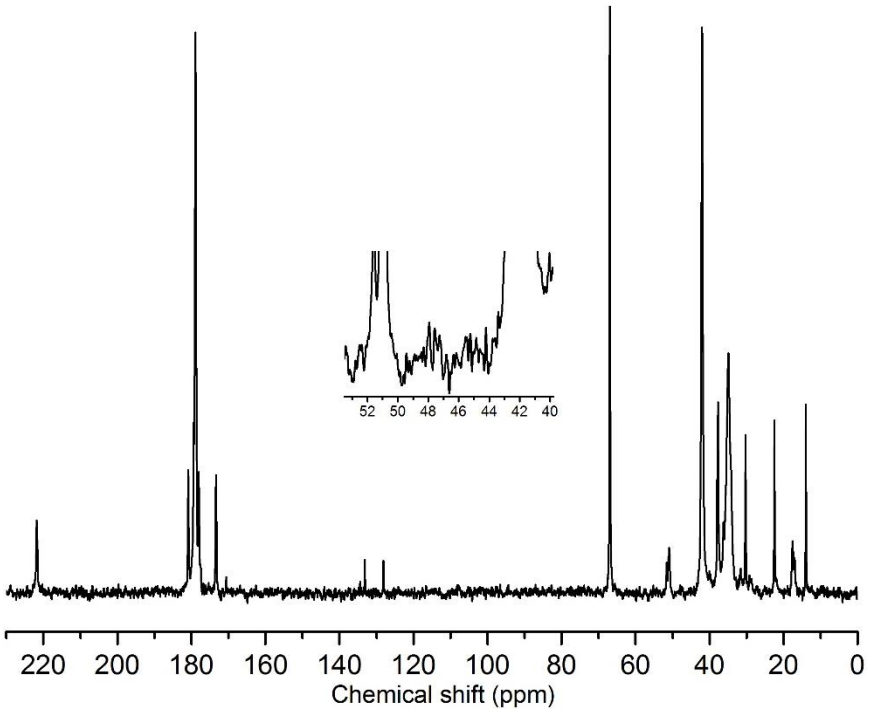

Figure S-24. Quantitative ^{13}C NMR spectrum of AA11 dissolved in D_2O obtained by an inverse-gated decoupling sequence. Insert shows region where the quaternary carbon from the branching point appears.

6.4 ^{1}H NMR spectra of oligoAA

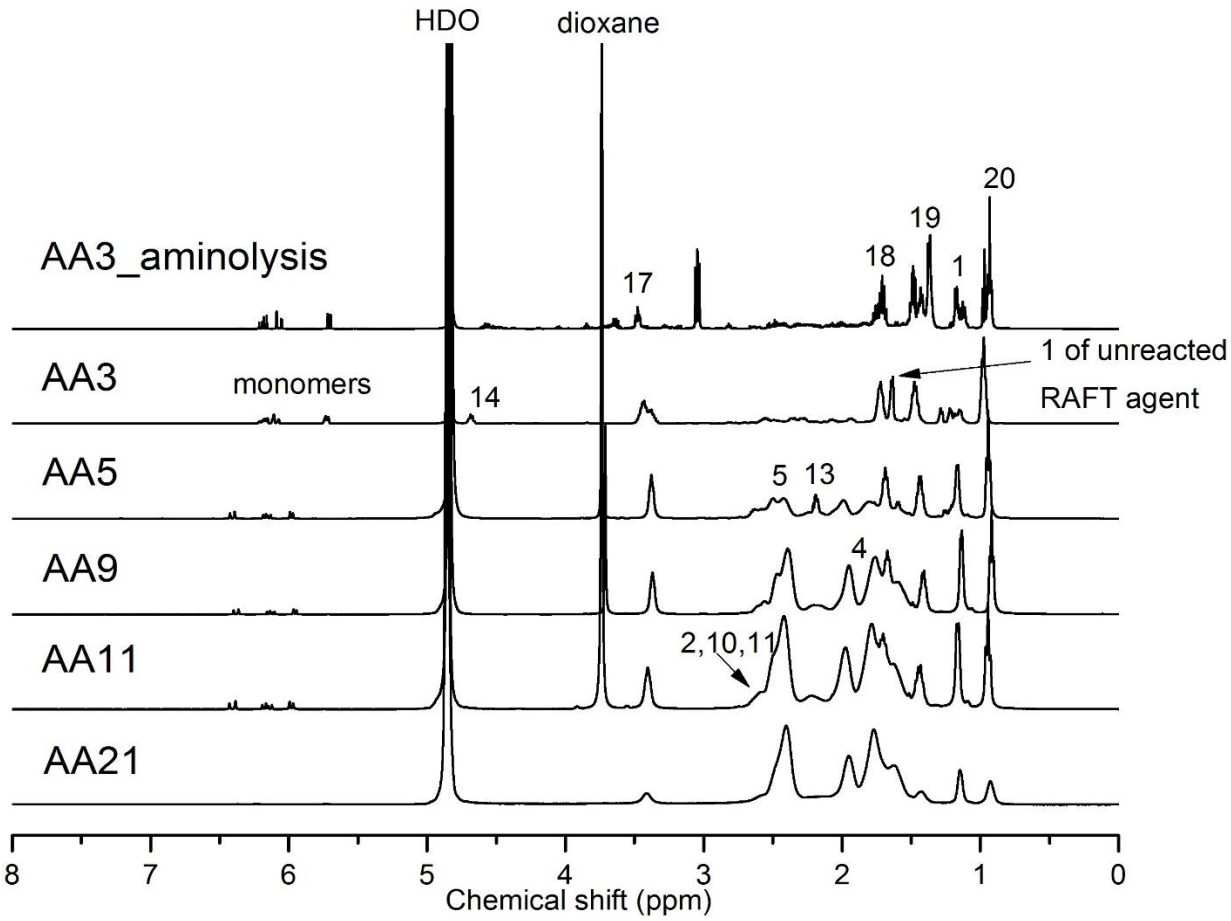

Figure S-25. ^{1}H NMR spectra of various oligoAA dissolved in D_2O. The top spectrum is of the AA3 sample after undergoing aminolysis. Numbers indicate the nuclei in the corresponding chemical structure shown in Figure 3.

6.5 ^{13}C NMR spectra of oligoAA

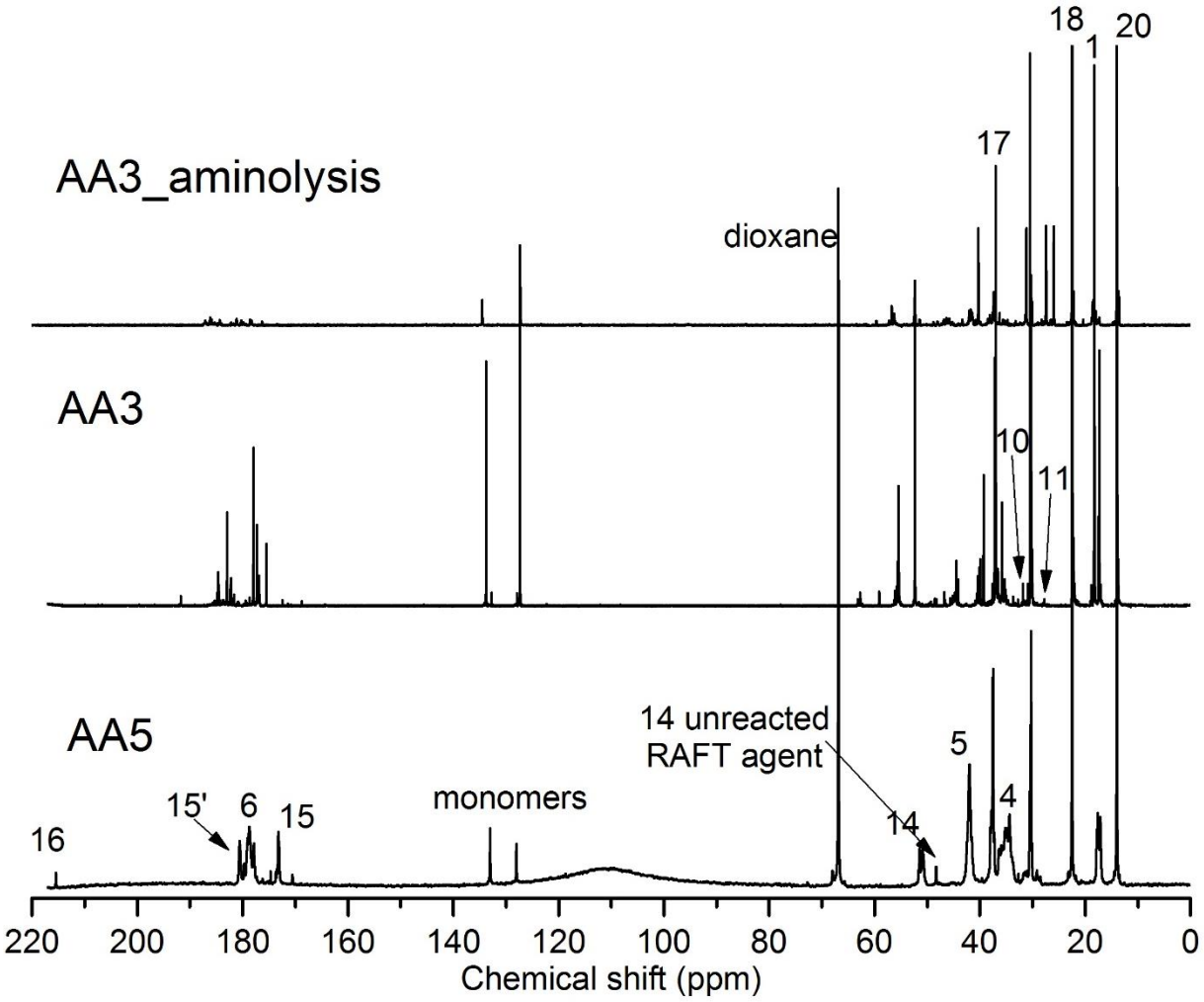

Figure S-26. ^{13}C NMR spectra of the small oligoAA samples dissolved in D_2O. The top spectrum is the AA3 sample after undergoing aminolysis. Numbers indicate the nuclei in the corresponding chemical structure shown in Figure 3.

6.6 2D NMR Spectra

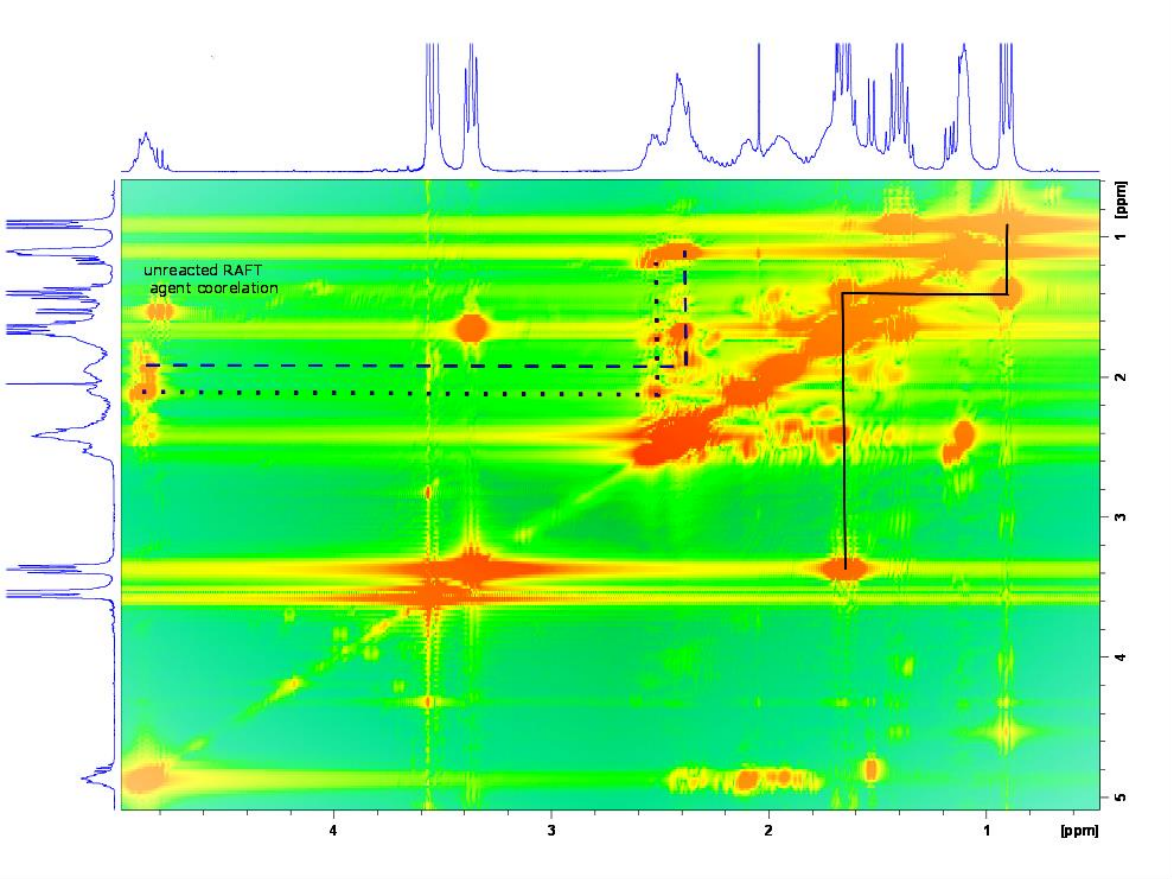

Figure S-27. ^{1}H-^{1}H COSY spectrum of AA4 dissolved in dioxane-d_8. The black line shows the correlations of the RAFT agent end group signals. The blue dashed line shows the correlations of the backbone signals. The purple dotted line shows the correlations of the monomer units next to the RAFT agent end group.

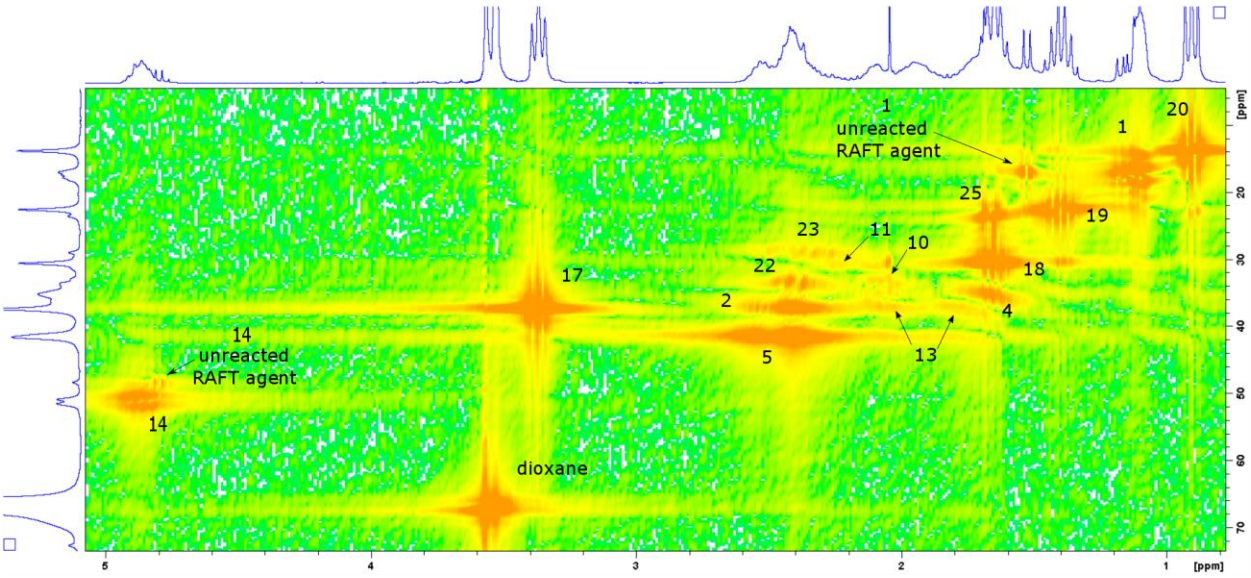

Figure S-28. ^{1}H-^{13}C HMQC spectrum of AA4 dissolved in dioxane-d_8. The numbers correspond to the nuclei labelled in Figure 3.

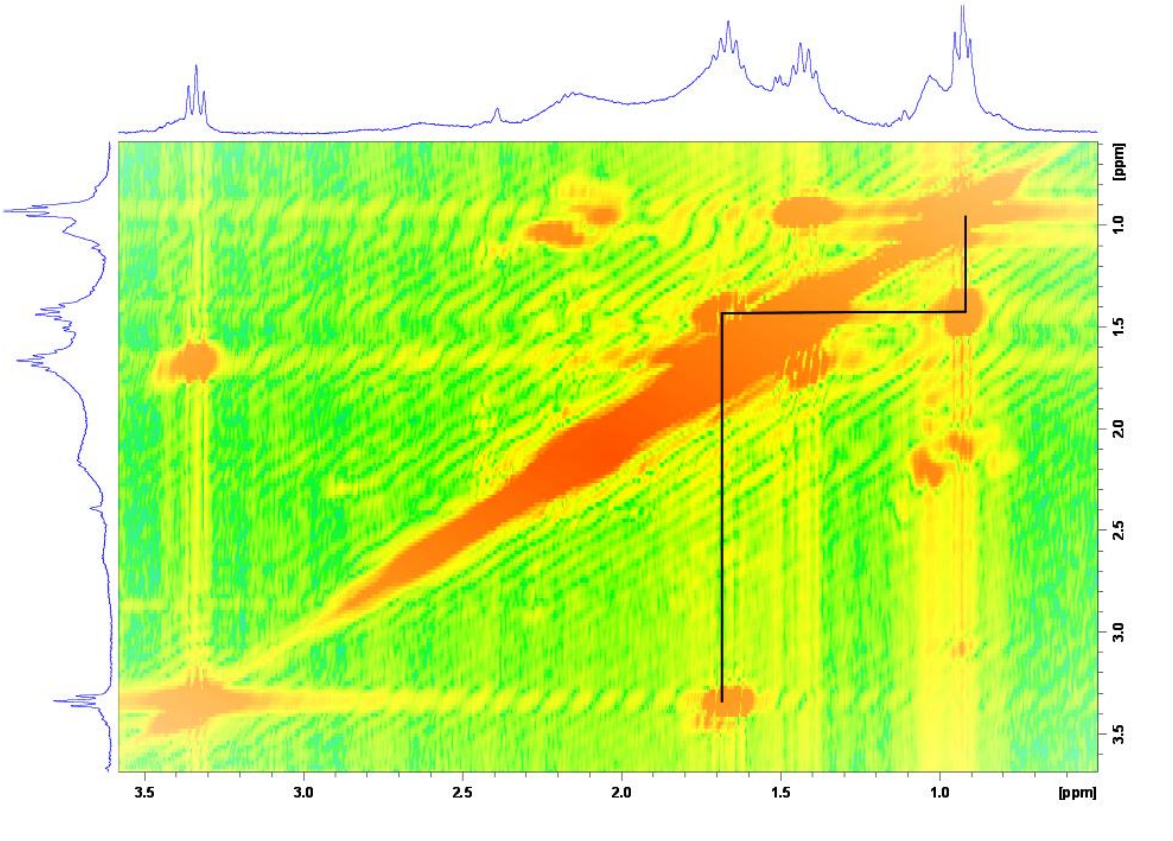

Figure S-29. ^{1}H-^{1}H COSY spectrum of AA4Sty2 dissolved in D_2O with 1 mol equivalent of NaOD. Black line shows the correlations of the RAFT agent end group signals.

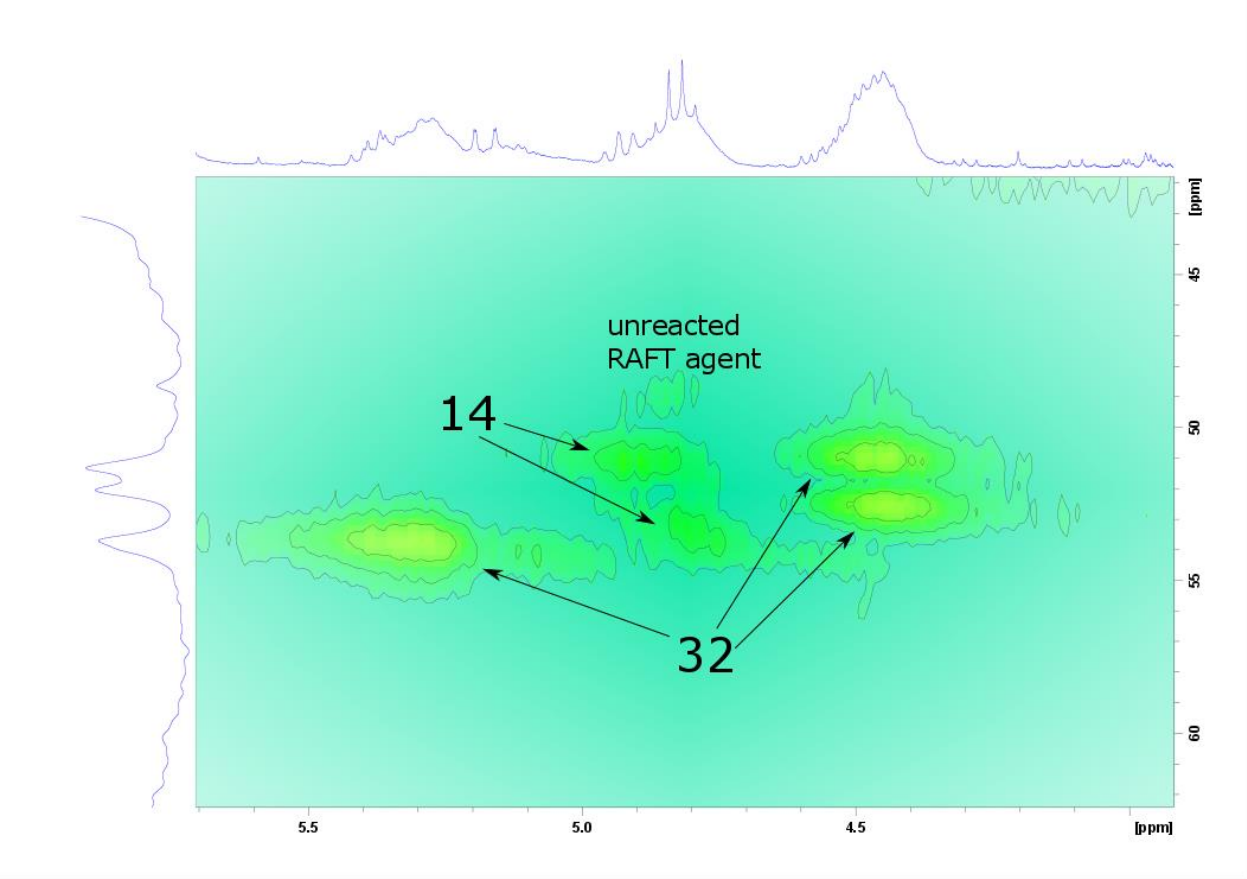

Figure S-30. ^{1}H-^{13}C HMQC spectrum of AA4Sty3 dissolved in THF-d^{8}. Numbers correspond to the nuclei labelled in Figure 3.

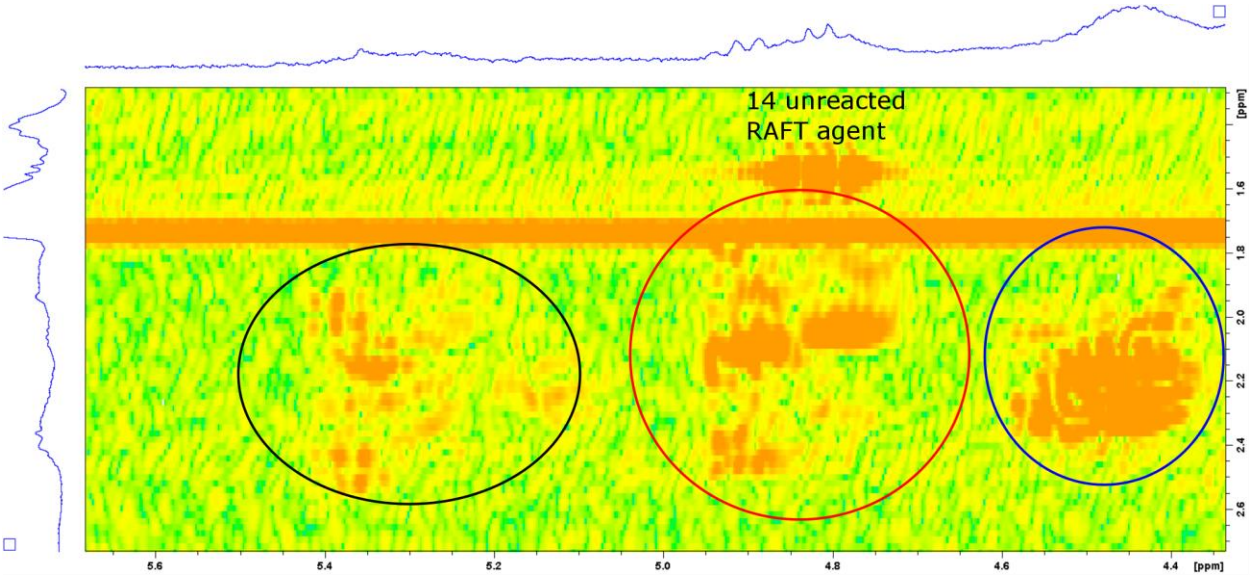

Figure S-31. ^{1}H-^{1}H COSY spectrum of AA4Sty3 dissolved in THF-d^{8}. Red circle identifies signals linked to AA units next to RAFT agent end group. Black and blue circles identify signals linked to Sty units next to RAFT agent end group.

7. References

[1] M. Adler, H. Pasch, C. Meier, R. Senger, H.G. Koban, M. Augenstein, G. Reinhold, Molar mass characterization of hydrophilic copolymers, 1 Size exclusion chromatography of neutral and anionic (meth)acrylate copolymers, E-Polymers, (2004).
[2] A. Dona, C.W.W. Yuen, J. Peate, R.G. Gilbert, P. Castignolles, M. Gaborieau, A new NMR method for directly monitoring and quantifying the dissolution kinetics of starch in DMSO, Carbohydr. Res., 342 (2007) 2604-2610.
[3] D. Nguyen, C. Such, B. Hawkett, Polymer-TiO_2 composite nanorattles via RAFT-mediated emulsion polymerization, J. Polym. Sci., Part A: Polym. Chem., 50 (2012) 346-352.
[4] D.E. Ganeva, E. Sprong, H. De Bruyn, G.G. Warr, C.H. Such, B.S. Hawkett, Particle formation in ab initio RAFT mediated emulsion polymerization systems, Macromolecules, 40 (2007) 6181-6189.
[5] C.J. Ferguson, R.J. Hughes, D. Nguyen, B.T.T. Pham, R.G. Gilbert, A.K. Serelis, C.H. Such, B.S. Hawkett, Ab initio emulsion polymerization by RAFT-controlled self-assembly, Macromolecules, 38 (2005) 2191-2204.
[6] M. Siauw, B.S. Hawkett, S. Perrier, Short chain amphiphilic diblock co-oligomers via RAFT polymerization, J. Polym. Sci., Part A: Polym. Chem., 50 (2012) 187-198.
[7] J. Chamieh, M. Martin, H. Cottet, Quantitative analysis in capillary electrophoresis: Transformation of raw electropherograms into continuous distributions, Anal. Chem., 87 (2015) 1050-1057.
[8] M.R. Toutounji, M.P. Van Leeuwen, J.D. Oliver, A.K. Shrestha, P. Castignolles, M. Gaborieau, Quantification of sugars in breakfast cereals using capillary electrophoresis, Carbohydr. Res., 408 (2015) 134-141.
[9] J.J. Thevarajah, A.T. Sutton, A.R. Maniego, E.G. Whitty, S. Harrisson, H. Cottet, P. Castignolles, M. Gaborieau, Quantifying the Heterogeneity of Chemical Structures in Complex Charged Polymers through the Dispersity of Their Distributions of Electrophoretic Mobilities or of Compositions, Anal. Chem., 88 (2016) 1674-1681.
[10] T. Kaneta, T. Ueda, K. Hata, T. Imasaka, Suppression of electroosmotic flow and its application to determination of electrophoretic mobilities in a poly(vinylpyrrolidone)-coated capillary, J. Chromatogr. A, 1106 (2006) 52-55.
[11] X.W. Yao, D. Wu, F.E. Regnier, Manipulation of electroosmotic flow in capillary electophoresis, J. Chromatogr. A, 636 (1993) 21-29.
[12] P. Castignolles, M. Gaborieau, E.F. Hilder, E. Sprang, C.J. Ferguson, R.G. Gilbert, High-resolution separation of oligo(acrylic acid) by capillary zone electrophoresis, Macromol. Rapid Commun., 27 (2006) 42-46.
[13] C.J. Evenhuis, W.C. Yang, C. Johns, M. Macka, P.R. Haddad, Fluorinated ethylenepropylene copolymer as a potential capillary material in CE, Electrophoresis, 28 (2007) 3477-3484.
[14] M.-F. Llauro, J. Loiseau, F. Boisson, F. Delolme, C. Ladavière, J. Claverie, Unexpected end-groups of poly(acrylic acid) prepared by RAFT polymerization, J. Polym. Sci., Part A: Polym. Chem., 42 (2004) 5439-5462.
[15] J.F. Lutz, K. Matyjaszewski, Nuclear magnetic resonance monitoring of chain-end functionality in the atom transfer radical polymerization of styrene, J. Polym. Sci., Part A: Polym. Chem., 43 (2005) 897-910.
[16] Y. Kwak, A. Goto, K. Komatsu, Y. Sugiura, T. Fukuda, Characterization of low-mass model 3-arm stars produced in reversible addition-fragmentation chain transfer (RAFT) process, Macromolecules, 37 (2004) 4434-4440.
[17] J.B. Lena, A.K. Goroncy, J.J. Thevarajah, A.R. Maniego, G.T. Russell, P. Castignolles, M. Gaborieau, Effect of transfer agent, temperature and initial monomer concentration on branching in poly(acrylic acid): A study by13C NMR spectroscopy and capillary electrophoresis, Polymer, 114 (2017) 209-220.

[18] K.L. Berkowski, S.L. Potisek, C.R. Hickenboth, J.S. Moore, Ultrasound-induced site-specific cleavage of azo-functionalized poly(ethylene glycol), Macromolecules, 38 (2005) 8975-8978.
[19] J. Loiseau, N. Doërr, J.M. Suau, J.B. Egraz, M.F. Llauro, C. Ladavière, J. Claverie, Synthesis and Characterization of Poly(acrylic acid) Produced by RAFT Polymerization. Application as a Very Efficient Dispersant of $CaCO_3$, Kaolin, and TiO_2, Macromolecules, 36 (2003) 3066-3077.
[20] C. Preusser, R.A. Hutchinson, An in-situ NMR study of radical copolymerization kinetics of acrylamide and non-ionized acrylic acid in aqueous solution, Macromol. Symp., 333 (2013) 122-137.
[21] D.R. Hensley, S.D. Goodrich, H. James Harwood, P.L. Rinaldi, 2D-Indequate NMR evidence for the termination mechanism of styrene free radical polymerization, Macromolecules, 27 (1994) 2351-2353.
[22] D.R. Hensley, S.D. Goodrich, A.Y. Huckstep, H. James Harwood, P.L. Rinaldi, 2D-Inadequate NMR evidence for the termination mechanism of styrene free-radical polymerization, Macromolecules, 28 (1995) 1586-1591.
[23] T.D.W. Claridge, High-Resolution NMR Techniques in Organic Chemistry, Introducing high-resolution NMR, 2nd ed., Elsevier2009, Chapter 2.
[24] D.J. Keddie, A guide to the synthesis of block copolymers using reversible-addition fragmentation chain transfer (RAFT) polymerization, Chem. Soc. Rev., 43 (2014) 496-505.
[25] V.P. Kartavykh, V.A. Drach, Y.N. Barantsevich, Y.L. Abramenko, Polymerization of diene hydrocarbons in the presence of azonitrile initiators containing carboxyl and hydroxyl groups, Polymer Science U.S.S.R., 19 (1977) 1413-1417.
[26] S.P. Vernekar, N.D. Ghatge, P.P. Wadgaoknar, Decomposition rate studies of azobisnitriles containing functional groups, J. Polym. Sci., Part A: Polym. Chem., 26 (1988) 953-958.
[27] P. Castignolles, R. Graf, M. Parkinson, M. Wilhelm, M. Gaborieau, Detection and quantification of branching in polyacrylates by size-exclusion chromatography (SEC) and melt-state 13C NMR spectroscopy, Polymer, 50 (2009) 2373-2383.